BIOCHEMICAL AND CELLULAR CHARACTERIZATION OF NMN ADENYLYLTRANSFERASE 2: A BRAIN SPECIFIC ISOFORM OF AN ESSENTIAL NAD SYNTHESIZING ENZYME

APPROVED BY SUPERVISORY COMMITTEE

Gang Yu, Ph.D.

Joachim Seemann, Ph.D.

Elliott Ross, Ph.D.

Jonathan Terman, Ph.D.

Russell DeBose-Boyd, Ph.D.

DEDICATION

First and foremost I thank my mentor Gang Yu. I have met few others with the same level of intellectual courage (and curiosity) who also retain the flexibility to be won over by well-reasoned counterarguments. I deeply appreciate his guidance and support. I also appreciate the guidance that I have received from my dissertation committee: Joachim Seemann, Elliott Ross, Jonathan Terman and Russell Debose-Boyd.

I thank my fellow lab members, especially the γ-secretase subgroup: Yu-Hong Han, Dan Dries, and Yun Wang. Science cannot be done in a vacuum and although my project had nothing to do with γ-secretase, they provided their full attention and support. Colleen Dewey, Basar Cenik and Chantelle Sephton also provided critical reagents, expertise and discussion. Cong Yu superbly managed the necessary day-to-day tasks that a busy lab requires.

Over the years, many scientists at UT Southwestern that have generously provided critical reagents and/or technical guidance; however, the following have been especially helpful: Hong Zhang, Nian Huang, Sanjiv Shah, Thomas Südhof, Anton Maximov, Pascal Kaeser, Katsuhiko Tabuchi, Gilbert Gallardo, Sandra Hofmann and Joachim Seemann.

Finally, I dedicate this work to my wife and son. None of this would have been possible without their love, support and nearly infinite patience. I have learned a great deal while working on this project. Much more than just the science presented here. For this, I am truly grateful.

BIOCHEMICAL AND CELLULAR CHARACTERIZATION OF NMN ADENYLYLTRANSFERASE 2; A BRAIN SPECIFIC ISOFORM OF AN ESSENTIAL NAD SYNTHESIZING ENZYME

by

PAUL ROBARDS MAYER III

DISSERTATION

Presented to the Faculty of the Graduate School of Biomedical Sciences

The University of Texas Southwestern Medical Center at Dallas

In Partial Fulfillment of the Requirements

For the Degree of

DOCTOR OF PHILOSOPHY

The University of Texas Southwestern Medical Center at Dallas

Dallas, Texas

December, 2010

BIOCHEMICAL AND CELLULAR CHARACTERIZATION OF NMN ADENYLYLTRANSFERASE 2; A BRAIN SPECIFIC ISOFORM OF AN ESSENTIAL NAD SYNTHESIZING ENZYME

PAUL ROBARDS MAYER III

The University of Texas Southwestern Medical Center at Dallas, 2010

GANG YU, Ph.D.

NMN adenylyltransferase 2 (Nmnat2) is one of three vertebrate enzymes that catalyze the synthesis of NAD from NMN and ATP. Nmnat1, -2 and -3 are each expressed from a separate gene and are distinguished from one another by their expression, subcellular localization and enzyme kinetics. Nmnat overexpression in neurons slows the rate of axon degeneration. This phenotype requires Nmnat activity and is caspase-independent suggesting that neuronal NAD metabolism regulates a novel program of self-destruction in axons. Nmnat2 is detected exclusively in the brain, unlike Nmnat1 and Nmnat3, which are widely expressed. Furthermore, Nmnat2 localizes to the Golgi complex in HeLa cells. Taken together, these observations suggest that Nmnat2 may have a specialized role in NAD metabolism in the brain. The goal of the work presented here is essentially to describe the molecular interactions of Nmnat2 and to attempt to understand what role Nmnat2 fulfills in the brain that cannot be met by Nmnat1 or Nmnat3. As described here, I have discovered that Nmnat2 is a neuronal peripheral membrane protein anchored via palmitoylation that localizes to dendrites and the cell body. Furthermore, I argue that a low level of Nmnat2 in the axon, or possibly its

exclusion altogether, is required for normal (i.e. fast) axon degeneration, providing a rationale for its membrane association and rapid turnover.

TABLE OF CONTENTS

PRIOR PUBLICATIONS

PR Mayer, N Huang, CM Dewey, DR Dries, H Zhang, and G Yu. (2010). Expression, localization and biochemical characterization of NMN adenylyltransferase 2. J Biol Chem *in press*. PMID: 20943658

CF Sephton, SK Good, S Atkin, CM Dewey, **P Mayer 3rd**, J Herz, and G Yu. (2010). TDP-43 is a developmentally regulated protein essential for early embryonic development. J Biol Chem *285*, 6826-6834. PMID: 20040602

TM Bricker, S Zhang, SM Laborde, **PR Mayer 3rd**, LK Frankel, and JV Moroney. (2004). The malic enzyme is required for optimal photoautotrophic growth of Synechocystis sp. strain PCC 6803 under continuous light but not under a diurnal light regimen. J Bacteriol 186, 8144-8148. PMID: 15547288

LIST OF FIGURES

LIST OF TABLES

LIST OF DEFINITIONS

Nmnat – NMN adenylyltransferase

NMN – nicotinamide mononucleotide

NAD – nicotinamide adenine dinucleotide

CHAPS – 3-[(3-cholamidopropyl)dimethylammonio]-1-propanesulfonic acid

LDS – lithium dodecyl sulfate

OG – octyl glucoside

MOI – multiplicity of infection

LHD – low homology domain

DRG – dorsal root ganglia

CHAPTER ONE:

INTRODUCTION

NAD Biosynthesis Pathways Converge on NMN Adenylyltransferase

Nicotinamide adenine dinucleotide (NAD) synthesis in eukaryotes can be divided into four pathways; each is defined by a unique set of enzymes that act on different precursors but ultimately converges on NMN adenylyltransferase (Belenky et al., 2007; Magni et al., 1999). Similar pathways are found in prokaryotes which also converge on NMN adenylyltransferase. Although NAD can be directly imported into cells, at least under certain conditions, it appears that most NAD is synthesized intracellularly (Billington et al., 2008; Haferkamp et al., 2004).

NMN adenylyltransferase (Nmnat) synthesizes NAD and pyrophosphate (PP_i) from nicotinamide mononucleotide (NMN) and adenosine triphosphate (ATP). The mechanism for this reaction is believed to occur via nucleophilic attack by the NMN phosphate on the ATP α-phosphate with PP_i acting as a leaving group (Lowe and Tansley, 1983; Saridakis et al., 2001). PP_i is rapidly hydrolyzed *in vivo* (Shatton et al., 1983), making this reaction effectively nonreversible under physiological conditions. In addition to NMN, Nmnat can also use nicotinic acid mononucleotide (NaMN) as a substrate (Dahmen et al., 1967; Preiss and Handler, 1958). This reaction yields nicotinic acid adenine dinucleotide (NaAD), which is subsequently converted to NAD by NAD synthetase.

In vertebrates, NMN is synthesized directly from either nicotinamide (Nam) or from nicotinamide riboside (Nr), a recently discovered precursor found in milk

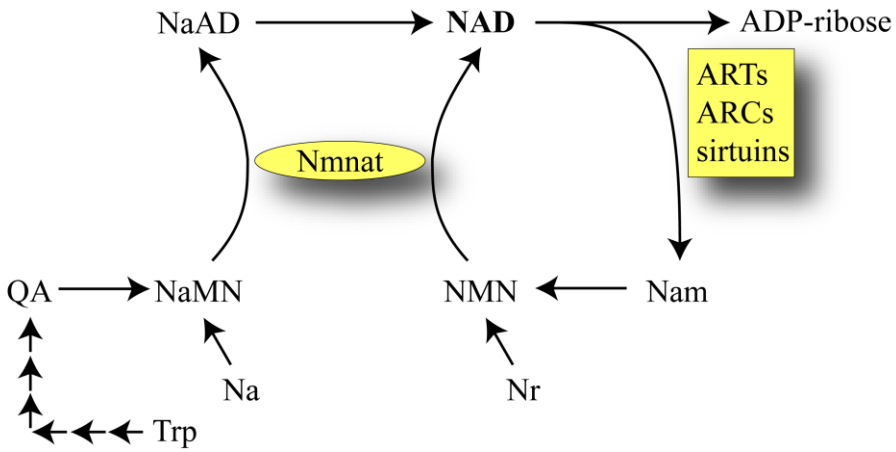

FIGURE 1.1 Vertebrate NAD Biosynthesis and Degradation Pathways. Vertebrates have four known NAD biosynthesis pathways. Each is defined by a unique set of enzymes acting of different precursors: *de novo* (Trp), Preiss-Handler (Na), salvage (Nam) and Nrk (Nr) pathways. All pathways converge on Nmnat. Trp, tryptophan; Na, nicotinic acid; Nam, nicotinamide; Nr, nicotinamide riboside; QA, quinolinic acid; NaMN, nicotinic acid mononucleotide; NMN, nicotinamide mononucleotide; NaAD, nicotinic acid adenine dinucleotide; ARTs, ADP-ribosyl transferases; ARCs, ADP-ribosyl cyclases.

(Bieganowski and Brenner, 2004) (FIGURE 1.1). The conversion of Nam to NMN to NAD is referred to as the salvage pathway. Since the conversion of Nrk to NMN requires a novel enzyme, this pathway is referred to as the Nrk pathway.

NaMN, alternatively, is synthesized directly from nicotinic acid (Na) or from tryptophan (Trp) through a multistep process (Belenky et al., 2007; Magni et al., 1999). The conversion of Na to NaMN to NaAD to NAD is referred to as the Preiss-Handler

pathway. NAD synthesis starting from Trp is referred to as the kynurenine (or *de novo*) pathway. Although the conversion of Trp to NAD is complex, requiring six different enzymes to generate NaMN, the last two steps of the Preiss-Handler and kynurenine pathways are the same.

In vertebrates, not surprisingly, NAD is synthesized from different precursors in different tissues (Shibata et al., 1986). All tissues can use nicotinamide (salvage), but the liver and kidney are also able to use tryptophan (kynurenine) and nicotinic acid (Preiss-Handler). The tissue expression of nicotinamide riboside kinase (Nrk), which converts Nr to NMN, has not been firmly established; however, Nrk is reported to be expressed in the heart and brain (Bogan and Brenner, 2008).

NAD Is a Cofactor and Consumable Substrate

NAD is a ubiquitous small molecule essential for life. A primary function of NAD (and NADP, its phosphorylated form) is to shuttle electrons between metabolic reactions. However, NAD is also used as a substrate, which results in cleavage of the glycosidic bond between nicotinamide and ADP-ribose. Nicotinamide is recycled to maintain cellular NAD levels, while the fate of ADP-ribose is reaction dependent. NAD consumers can be divided into three groups: ADP- ribosyl transferases (ARTs), ADP-ribosyl cyclases (ARCs) and sirtuins (Hottiger et al., 2010; Houtkooper et al., 2010; Koch-Nolte et al., 2009).

ARTs use NAD as an ADP-ribose donor, primarily for post-translational modification of proteins (Hottiger et al., 2010). Poly-ADP-ribose polymerase 1 (PARP1), which is the founding member of the PARP subfamily of ARTs, uses NAD to

synthesize long, branched chains of ADP-ribose on itself and other nuclear proteins (Krishnakumar and Kraus, 2010). PARP1-dependent ADP-ribosylation appears to play an important role in signaling pathways that regulate DNA repair and transcription, but its precise function is unclear. Similarly, the precise cellular function of other PARPs is also unclear. Excessive PARP activity due to massive DNA damage, however, results in the depletion of cellular NAD pools resulting in cell death (Berger, 1985; Yu et al., 2002).

Cyclic ADP-ribose (cADPR) is synthesized from NAD by CD38 and functions as a second messenger in calcium signaling (Schuber and Lund, 2004). CD38 knockout mice show decreased oxytocin release which correlates with abnormal social behavior (Jin et al., 2007). Interestingly, ARC activity has been detected in CD38 knockout mouse brain synaptosomes, although the source of this activity remains unknown (Ceni et al., 2006).

Sirtuins are class III deacetylases that transfer an acetyl group from specific protein targets to the ADP-ribose portion of NAD resulting in the release of nicotinamide and O-acetyl-ADP-ribose (Smith et al., 2008). Acetylation is a common reversible post-translational modification that regulates the function of a growing list of proteins (Choudhary et al., 2009). Mammals have seven sirtuins (SIRT1-7) that regulate diverse cellular functions (Finkel et al., 2009) including key metabolic pathways such as fatty-acid oxidation (Hirschey et al., 2010) and glucose metabolism (Rodgers et al., 2005; Zhong et al., 2010).

Are Sirtuins Regulated by Physiological Fluctuations of Intracellular NAD Concentrations?

Sirtuins are the only class of deacetylases that require NAD (Hildmann et al., 2007). This has prompted speculation that sirtuins are directly regulated by cellular NAD levels (Imai et al., 2000; Revollo et al., 2004; Schwer and Verdin, 2008; Yang et al., 2007; Yu and Auwerx, 2009). Two possible mechanisms to explain how sirtuins might function as NAD sensors are that 1) intracellular NAD concentrations vary dramatically (e.g. 10-fold) above and below sirtuin Michaelis constants (K_m^{NAD}) or 2) sirtuin substrate binding is cooperative. Unfortunately, a rigorous analysis of the K_m^{NAD} of mammalian SIRT1-7 has not been published and reported values vary significantly. Nonetheless, in general, SIRT1-7 appear to have K_m^{NAD} values between 0.1-0.5 mM (Sauve, 2010), while total cellular NAD is approximately 0.3 mM in mammalian cells (Yamada et al., 2006; Yang et al., 2007). However, *in vivo* NAD levels vary modestly under physiological conditions, approximately 2-fold or less (Nakahata et al., 2009; Ramsey et al., 2009; Rodgers et al., 2005; Yang et al., 2007), and there is no indication in the literature that sirtuin substrate binding is cooperative. Under these conditions, it is unlikely that sirtuins are regulated solely by NAD. Alternatively, it is possible that Nmnat regulates sirtuin activity through either substrate channeling or dramatically increasing the local concentration of free NAD. Data supporting this type of regulation has recently been published (Zhang et al., 2009). Others contend that sirtuins are regulated via inhibition by nicotinamide (Sauve et al., 2005) or NADH (Lin et al., 2004).

In addition to their dependence on NAD, sirtuins are also regulated through protein interaction, phosphorylation and sumoylation (Smith et al., 2008). Given the

central role of NAD in metabolic reactions, sirtuin-dependent deacetylation, and the role of sirtuins in the regulation of metabolic pathways, it is tempting to speculate that sirtuins are NAD sensors that are tuned to the metabolic state of the cell and respond accordingly. Although plausible, the mechanism for how this occurs remains to be determined. Nonetheless, it is likely that sirtuin regulation in mammals is complex and involves several different mechanisms including NAD availability.

Nmnat Overexpression Slows the Rate of Axon Degeneration (Wallerian Degeneration)

Wallerian degeneration (WD) is the programmatic self destruction of severed or crushed axons (Griffin et al., 1995; Waller, 1850). This process was initially thought to be passive, but a remarkable observation in a naturally occurring mutant mouse line reversed this assumption; after cutting the sciatic nerve, severed axons degenerated at a dramatically slower rate than normal (Lunn et al., 1989; Perry et al., 1990; Raff et al., 2002). *In vivo*, transected axons are capable of conducting action potentials for only a couple of days after injury (at most); however, severed axons from these mutant mice remained viable and were able to conduct action potentials for up to two weeks (Lunn et al., 1989; Perry et al., 1990). Although this discovery was made more than twenty years ago, the mechanism remains poorly understood.

C57BL/Ola mice, typically referred to as Wallerian degeneration slow (Wld^S) mice, have an 85kb tandem triplication (Coleman et al., 1998) located on the distal end of chromosome 4 (Lyon et al., 1993). As a result, these mice have two copies of a novel gene consisting of the 5'-UTR/N-terminal coding region for *Ufd2a* fused to the entire

coding region of *Nmnat1* (Conforti et al., 2000; Mack et al., 2001). Expression of this chimera results in a protein consisting of the first 70 amino acids from Ufd2a, a ubiquitin ligase (Kaneko et al., 2003), in frame with full length Nmnat1, one of three NMN adenylyltransferases expressed in vertebrates (see below) (Lau et al., 2009; Magni et al., 2004).

Subsequent experiments have revealed that overexpression of Nmnat in neurons is sufficient to initiate slow Wallerian degeneration (Press and Milbrandt, 2008; Sasaki et al., 2006; Yan et al., 2009) and more recent data indicates that Nmnat activity within the axon is essential for this phenotype (Babetto et al., 2010; Sasaki and Milbrandt, 2010).

A common theme among many neurodegenerative diseases is that axon "dying back" often precedes death of the neuronal cell body (Raff et al., 2002). Consequently, some of the symptoms associated with these diseases may be attributable to axon degeneration and not necessarily cell body death *per se*. Notably, regulation of axon destruction is caspase independent (Finn et al., 2000; Ikegami and Koike, 2003; Whitmore et al., 2003). A better understanding of neuronal NAD biology may provide insight into the mechanism of Nmnat-mediated slow axon degeneration.

Specialization of NMN adenylyltransferases in Vertebrates

Vertebrates express three different proteins with NMN adenylyltransferase activity: Nmnat1, Nmnat2 and Nmnat3 (Lau et al., 2009; Magni et al., 2004). Although each catalyzes the same reaction, albeit with different kinetic properties (Sorci et al., 2007), each is characterized by a unique expression pattern and subcellular localization

(Lau et al., 2009). This suggests that Nmnat1, -2 and -3 have evolved specialized roles in vertebrate NAD metabolism.

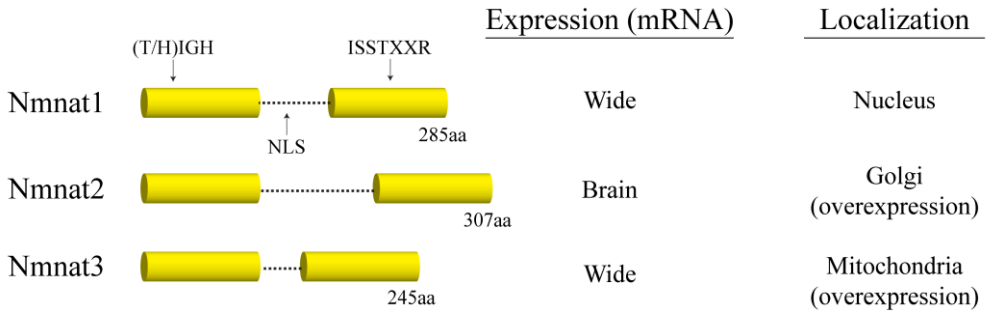

FIGURE 1.2 Properties of Human Nmnat Family. Nmnat1, -2 and -3 consist of a bipartite Rossmann fold linked by a poorly conserved region referred to here as the low homology domain (LHD); denoted by *dotted line* (conserved regions are in yellow). The LHD is not resolved in the crystal structure for Nmnat1 and Nmnat3 (structure of Nmnat2 is not published) suggesting that this region is flexible. The nuclear localization sequence (NLS) for Nmnat1is contained within this region. (T/H)IGH and ISSTXXR are conserved substrate binding motifs found in all NMN adenylyltransferases.

Unlike Nmnat1 and Nmnat3, which are widely expressed although not necessarily overlapping (Lau et al., 2009), Nmnat2 transcript is expressed predominately in the brain (Raffaelli et al., 2002; Sood et al., 2001; Yalowitz et al., 2004). Furthermore, Nmnat2 localizes to Golgi (Berger et al., 2005), while Nmnat1 is nuclear (Berger et al., 2005; Hogeboom and Schneider, 1952) and Nmnat3 associates with mitochondria (Berger et al., 2005; Zhang et al., 2003).

Summary

It is unknown what function Nmnat2 fulfills in the brain that cannot be met by Nmnat1 or Nmnat3. The purpose of the research presented here is to characterize the expression, localization, biochemistry and cellular/physiological function of Nmnat2.

Furthermore, it is anticipated that this data will provide insight into the mechanism of Nmnat-dependent slow Wallerian degeneration.

CHAPTER TWO:

CELLULAR AND BIOCHEMCIAL

CHARACTERIZATION OF NMNAT2

Abstract

NMN adenylyltransferase 2 (Nmnat2) catalyzes the synthesis of NAD from NMN and ATP. Nmnat2 transcript is expressed predominately in the brain; we report here that Nmnat2 is a low abundance protein expressed in neurons. Previous studies indicate that Nmnat2 localizes to Golgi. Since Nmnat2 is not predicted to contain a signal sequence, lipid-binding domain or transmembrane domain, we investigated the nature of this interaction. These experiments reveal that Nmnat2 is palmitoylated *in vitro* and this modification is required for membrane association. Surprisingly, exogenous Nmnat2 is toxic to neurons indicating that protein levels must be tightly regulated. To analyze Nmnat2 localization in neurons (previous experiments relied on exogenous expression in HeLa cells), mouse brains were fractionated showing that Nmnat2 is enriched in numerous membrane compartments including at synaptic terminals. In HeLa cells, in addition to Golgi, Nmnat2 localizes to Rab7-containing late endosomes. These studies show that Nmnat2 is a neuronal protein peripherally attached to membranes via palmitoylation and suggest that Nmnat2 is transported to synaptic terminals via an endosomal pathway.

Introduction

NMN adenylyltransferases (Nmnat) catalyze the synthesis of NAD from NMN and ATP (Lau et al., 2009; Magni et al., 1999; Magni et al., 2008). Humans and mice express three isoforms, each from a separate gene: *Nmnat1*, *-2* and *-3*; while invertebrates such as *D. melanogaster* have only one (Zhai et al., 2006). Nmnat2 is unique in that its transcript is expressed predominately in the brain (Raffaelli et al., 2002; Sood et al., 2001; Yalowitz et al., 2004). In contrast, Nmnat1 and -3 transcripts are widely expressed although not necessarily overlapping (Magni et al., 2008). Furthermore, Nmnat2 localizes to Golgi (Berger et al., 2005), while Nmnat1 is nuclear (Berger et al., 2005; Hogeboom and Schneider, 1952) and Nmnat3 associates with mitochondria (Berger et al., 2005; Zhang et al., 2003). This suggests that: [1] Nmnat1, -2 and -3 have evolved specialized roles in vertebrate NAD metabolism and [2] the subcellular location of NAD synthesis is cell-type specific.

In addition to its role as a cofactor, NAD is also a substrate for numerous enzymes including sirtuins, poly(ADP-ribose) polymerases (PARPs) and ADP-ribosyl cyclases (e.g. CD38) (Belenky et al., 2007). These enzymes regulate diverse cellular processes including transcription, apoptosis and calcium signaling (Finkel et al., 2009; Graeff et al., 2009; Kraus, 2008). In eukaryotes, NAD is synthesized either *de novo* from tryptophan or recycled from nicotinic acid, nicotinamide or nicotinamide riboside (Belenky et al., 2007; Magni et al., 1999). Because neurons require an enormous amount of energy to propagate action potentials, it is not surprising that insufficient dietary intake of NAD-precursors results in severe neurological dysfunction (Hegyi et al., 2004; Spies et al., 1939).

It is unclear what specific role Nmnat2 has in the brain that cannot be met by Nmnat1 or -3. To address this question, we have first sought to understand how Nmnat2 interacts with the Golgi, its cellular and developmental protein expression, and its localization in brain cells. We report here that Nmnat2 is a developmentally regulated, low abundance neuronal protein that localizes not only to Golgi but also to vesicles and synaptic compartments. Overexpression of Nmnat2 is toxic to neurons, suggesting that endogenous protein levels must be tightly regulated and providing a rationale for its low abundance. Additional experiments investigate its interaction with Golgi revealing that Nmnat2 is peripherally attached to the membrane via palmitoylation. Biochemical analysis shows that *endogenous* Nmnat2 behaves like a membrane protein but is difficult to solubilize suggesting that: [1] palmitoylation directs Nmnat2 to detergent resistant membranes or [2] in addition to palmitoylation Nmnat2 is held at the membrane via protein-protein interaction. Finally, colocalization studies in HeLa cells suggest that Nmnat2 may traffic through an endosomal pathway via Rab7-containing vesicles. The data presented here provide the basis for future investigation of the specific role of Nmnat2 in neuronal NAD metabolism.

Methodology

Antibodies

Full-length human Nmnat2 (NM_015039) was cloned into pET-28a (Novagen) and expressed in Rosetta (DE3)pLysS Escherichia coli. The resulting His-tag fusion protein was purified using Ni-NTA agarose beads (Qiagen) according to the manufacturer's guidelines. Polyclonal antibody was generated by YenZym Antibodies

(South San Francisco, CA) and purified by affinity chromatography. Antibodies against the following proteins were purchased from the indicated vendors: NF, heavy chain (Affinity BioReagents); VCP and GM130 (BD Biosciences); Rab7 and EEA1 (Cell Signaling Technology); EEA1, FLAG, GAPDH, TGN46 and VDAC (Sigma). Antibodies against Rab5, Syb 2, Syt I and α/β-NRX were kindly donated by Thomas Südhof (Stanford School of Medicine, Palo Alto, CA). Joachim Seemann (UT Southwestern Medical Center, Dallas, TX) kindly donated anti-β-COP antibody.

Mammalian expression vectors, and site-directed mutatagenesis

Human Nmnat2(NM_015039) was cloned into pEGFP-N1 (Clontech) as previously described (Zhang et al., 2003). This construct is referred to here as Nmnat2-EGFP and was used as template for PCR-based mutagenesis to create the C164S/C165S mutant as well as the LHD (see below) deletion mutants. Nmnat2-FLAG and Nmnat2 C164S/C165S-FLAG were generated by subcloning into a C-terminal FLAG vector. All constructs were verified by DNA sequencing.

Lentivirus production

Lentiviral shRNA vectors (pLKO.1-puro) targeted against mouse Nmnat2 and EGFP were purchased from Sigma. Nmnat2-EGFP and its derivatives were subcloned into a modified version of FUGW, a lentivirus expression vector, which along with the packaging constructs pVSVG and pCMVΔ8.9, were kindly provided by Thomas Südhof (Stanford School of Medicine, Palo Alto, CA). Lentiviruses were produced from HEK293T triple-transfected (Fugene 6) with pVSVG, pCMVΔ8.9 and one of the

lentiviral expression vectors described above. Approximately 48 h after transfection, virus containing media was collected and filtered (0.45 μm) then stored in small aliquots at -80 °C until needed. Viruses were tittered by quantitative PCR (qPCR) (Salmon and Trono, 2006; Sastry et al., 2002).

Cell culture and imaging

HEK293T, Neuro-2a (N2a) and SH-SY5Y cell lines were purchased from ATCC. U343 and U87 cells were generously donated by Richard Lu (UT Southwestern Medical Center, Dallas, TX). HeLa cells were a gift from Joachim Seemann (UT Southwestern Medical Center, Dallas, TX). Cultures were maintained in growth media containing 10 % FBS/D-MEM (Invitrogen), except SH-SY5Y, which were maintained in 10 % FBS/Advanced-MEM supplemented with non-essential amino acids, 110 mg/ml sodium pyruvate and 2 mM glutamine (Invitrogen). SH-SY5Y cells were differentiated using a previously established protocol (Encinas et al., 2000). In brief, SH-SY5Y were seeded at low density and sequentially treated with 10 μM retinoic acid (Sigma) in growth media for 5 d and then 50 ng/ml human BDNF (Invitrogen) in serum-free media for an additional 7 d. At this point, most cells developed a rounded shape with an extensive network of neurites emanating from clumps of cell bodies.

Primary neuronal cultures were generated using standard procedures from cortex dissected from late embryonic (E18) mouse brains. In brief, tissues were cut into small uniform pieces and treated for ~5 min with warm papain solution (20 units/mL, Worthington; dissolved in HBSS supplemented with 10 mM HEPES-NaOH, pH ~7.2, Invitrogen). To inactivate the papain, tissue fragments were briefly incubated with a

solution of 1.25 % trypsin inhibitor (Sigma), then rinsed with cold HBSS/HEPES buffer. Neurons were dissociated by gentle trituration using a fire-polished Pasteur pipette in neuronal growth media: Neurobasal supplemented with B-27 and 2 mM glutamine (Invitrogen). For expression analysis, cells were plated on poly-D-lysine (0.1 mg/ml, Sigma) coated 6 cm dishes at a density of 1 x 10^6 cells/plate. Neurons were fed every 3 d and collected at various timepoints, as indicated. Primary glia cultures were also derived from the cortex using a similar procedure with the following exceptions: tissue fragments were incubated with papain solution for 15 min and cultures were maintained in 10 % FBS/D-MEM. The absence of neurotrophic factors results in the selective loss of neurons. Glial cultures were fed every 7 d and were maintained for ~21 d before harvesting.

For immunofluorescence experiments, cortical neurons were seeded at a density of 1 x 10^5 cells per coverslip (12 mm diameter, Fisher Scientific) previously treated with Matrigel (1:100 in PBS, BD Biosciences) and 0.1 mg/ml poly-D-lysine (Sigma). HeLa were seeded at a density of 2 x 10^4 cells per coverslip. Cells were fixed with 3.7 % paraformaldehyde (PFA) and permeablized with 0.1 % Triton X-100, then washed several times with PBS and blocked for 30 min with a solution of 4 % BSA (Sigma) and 1 % normal goat serum (Jackson ImmunoResearch). Incubation with primary antibody was done overnight at 4 °C. Coverslips were mounted with ProLong Gold antifade reagent (Invitrogen) and images were collected using a Zeiss LSM 510 confocal microscope.

Analysis of Nmnat2 expression in cells and tissue

Tissues were collected from age-matched mice and washed with PBS and then immediately flash-frozen in liquid nitrogen and ground to powder using a mortar and pestle. Cells were washed with ice-cold PBS then collected with a rubber policeman and centrifuged at 400 x g for 5 min. Cell pellets and tissue powder were lysed with cold 50 mM HEPES-NaOH, 1 % LDS, 1 mM DTT and protease inhibitors (0.2 mM PMSF, 0.5 μg/ml leupeptin and 1 μM pepstatin A) and then briefly sonicated to reduce viscosity. Protein concentration was measured using the DC protein assay according to manufacturer's instructions (Bio-Rad). Within a given experiment, the same amount of total protein was loaded for each sample.

Palmitoylation Assay

HEK293T cells transiently expressing Nmnat2-FLAG or Nmnat2 C164S/C165S-FLAG were incubated for 6 h in media containing 0.4 mCi/ml [9,10-^{3}H(N)]-palmitic acid (Perkin Elmer). Cells were washed with ice-cold PBS, collected using a rubber policeman and centrifuged at 800 x g, then lysed with 1 % LDS/4 M urea and diluted 1:20 with buffer B (1 % NP-40, 0.2 mM PMSF, 0.5 μg/ml leupeptin and 1 μM pepstatin A). Diluted lysate was incubated with anti-FLAG agarose beads overnight at 4 °C. After extensive washing with PBS, bound protein was eluted in a small volume of sample buffer (60 mM Tris-HCl, pH 6.8, 2 % LDS, 10 % glycerol and 0.025 % bromophenol blue). Eluted protein was separated by SDS-PAGE and exposed to Biomax XAR film (Kodak) at -80 °C for 14 d. To enhance detection of radiolabeled protein, polyacrylamide gels were impregnated with 2,5-diphenyloxazole (Sigma) as described by Bonner and Laskey (Bonner and Laskey, 1974).

Purification and activity of Nmnat2 and Nmnat2 C164S/C165S

The coding sequence for human Nmnat2 and Nmnat2 C164S/C165S was cloned into pMBP-parallel1 (Sheffield et al., 1999). The resulting maltose-binding protein (MBP) fusion protein was affinity purified using amylose resin (New England BioLabs). After removal of the MBP tag by TEV protease treatment, Nmnat2 and Nmnat2 C164S/C165S were further purified using a Phenyl Sepharose column and finally by gel filtration chromatography (GE Healthcare).

Steady–state kinetic parameters were determined using a coupled assay adapted from Kurnasov et al. (Kurnasov et al., 2002). Briefly, reaction mixtures were prepared in parallel containing 50 mM HEPES-NaOH (pH 7.5), 115 mM ethanol, 40 mM semicarbazide, 6 units/ml of alcohol dehydrogenase, 5 % glycerol and varying amounts of ATP and NMN. Reactions were started by adding purified Nmnat2 or Nmnat2 C164S/C165S to a final concentration of 0.4 nM. The production of NADH was monitored by measuring absorbance at 340 nm. Apparent values of K_M and k_{cat} were calculated using SigmaPlot 11 (Systat Software).

Extraction of post-nuclear membrane (PNM) fractions

Whole mouse brains from adult mice were cut into equal size pieces and homogenized on ice using a glass-Teflon homogenizer (PEH) in buffer A supplemented with 320 mM sucrose. Buffer A consists of 10 mM HEPES-NaOH, pH 7.4, 1 mM DTT and protease inhibitors (0.2 mM PMSF, 0.5 μg/ml leupeptin and 1 μM pepstatin A). To reduce nuclear and whole cell contamination, homogenate was filtered through four

layers of cheesecloth and centrifuged at 900 x g for 10 min. The resulting supernatant was centrifuged at 100,000 x g for 1 h. The supernatant from this spin is designated as the cytosolic (S100) fraction. The pellet (P100), which is enriched for cytoplasmic membranes, was suspended with buffer A/320 mM sucrose. 100 µl aliquots of P100 (1 mg/ml) were centrifuged at 100,000 x g for 1 h. The resulting pellets were suspended in 100 µl of buffer A supplemented with of the following: 320 mM sucrose, 1 M NaCl, 4 M urea, 1 % CHAPS, 1 % octyl glucoside or 1 % LDS. Suspensions were incubated on ice for 30 min, and then centrifuged at 100,000 x g for 1 h. To analyze the hydrophobicity of endogenous Nmnat2, cytoplasmic membranes were extracted with 2 % Triton X-114 (EMD Chemicals) overnight on ice. Separation of the detergent and aqueous phases was done essentially as described by Brusca and Radolf (Brusca and Radolf, 1994).

Fractionation of mouse brain synaptosomes

This protocol is based on previously published methods with some modifications (Butz et al., 1999; Jones and Matus, 1974; Maximov et al., 2007; Whittaker et al., 1964). Whole mouse brains were homogenized in 320 mM sucrose, 10 mM HEPES-NaOH, pH 7.4, 1 mM DTT and protease inhibitors (0.2 mM PMSF, 0.5 µg/ml leupeptin and 1 µM pepstatin A) using a glass-Teflon homogenizer attached to an overhead motor (~500 RPM). Homogenate was filtered through four layers of cheesecloth and then centrifuged at 900 x g for 10 min to sediment nuclei and unbroken cells (P1). To enrich for synaptosomes and mitochondria, post-nuclear supernatant (S1) was centrifuged at 11,000 x g for 15 min. All remaining membranes in the resulting supernatant (S11) were

collected by centrifugation at 200,000 x g for 2 h (P200). The synaptosome/mitochondria pellet (P11) was washed once with homogenization buffer, and then lysed in hypotonic buffer (5 mM HEPES-NaOH, pH 7.4 supplemented with protease inhibitors). This suspension was then centrifuged at 25,000 x g for 20 min to sediment large membrane fragments (LP1). These membranes (LP1) were further fractionated by flotation through a discontinuous sucrose gradient. The LP1 pellet was suspended with 1.1 M sucrose and formed the bottom layer, with solutions of 0.855 M and 0.32 M sucrose layered on top. Gradients were centrifuged at 19,500 RPM for 2.5 h using an SW-41 rotor (Beckman Coulter). Myelin enriched membranes (A) were collected from the 0.32 M/0.855 M interface and synaptic plasma membranes (B) from the 0.855 M/1.1 M interface. Mitochondria accumulated at the bottom of the tube in a sticky dark brown pellet (C). Synaptosome supernatant (LS1) was centrifuged at 200,000 x g for 2 h to sediment synaptic and other small vesicles (LP2).

Results

Expression Profile of Nmnat2 Protein

To evaluate the expression of endogenous Nmnat2, we generated several polyclonal antibodies using either peptides or full-length protein. Following an initial assessment, sera against full-length Nmnat2 was chosen for further analysis. To establish its specificity, we looked for cell lines expressing high levels of Nmnat2 transcript (http://biogps.gnf.org/). As a result, Neuro-2a (N2a) cells, which are a mouse neuroblastoma cell line, were infected with three different shRNA-expressing lentiviruses: two targeted against Nmnat2 and one targeted against EGFP (negative

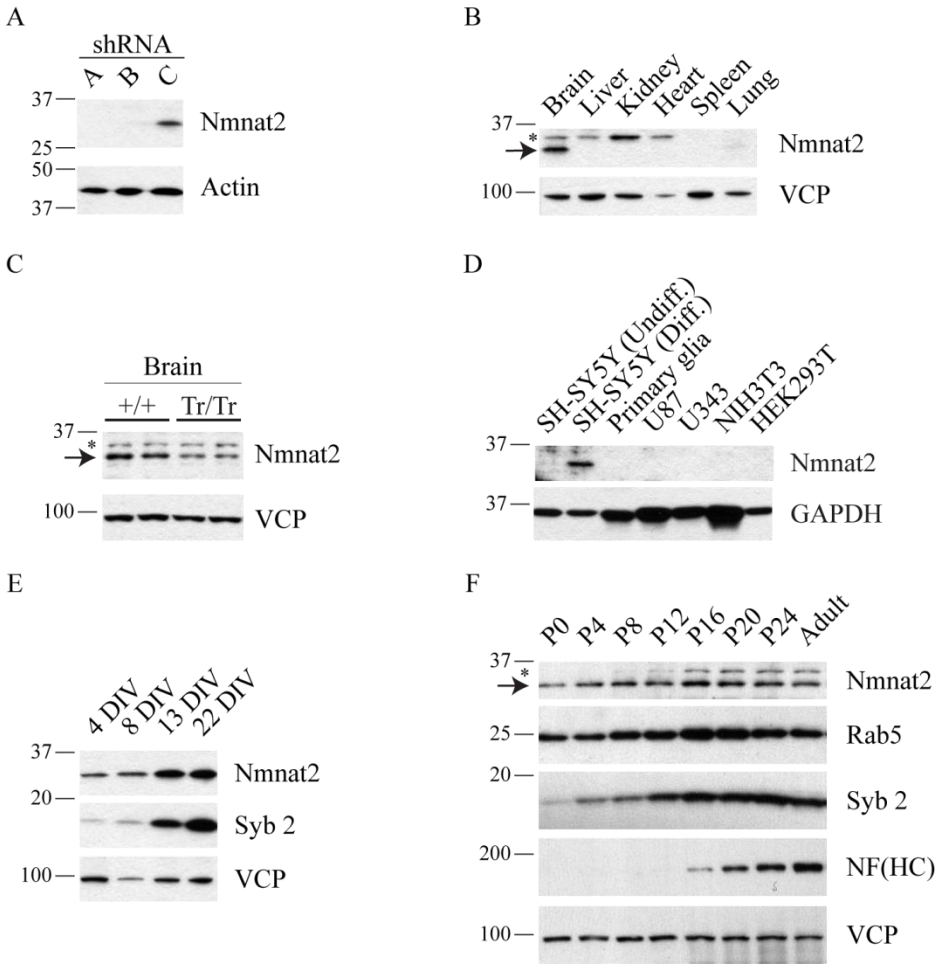

FIGURE 2.1 Nmnat2 Is a Neuronal Protein and Expression Is Developmentally Regulated. A, To assess the specificity of an in-house antibody targeted against full-length Nmnat2, N2a—a neuroblastoma cell line reported to express *Nmnat2* transcript (http://biogps.gnf.org)—were infected with lentiviruses (MOI = 1) expressing either shRNA against Nmnat2 (A and B) or EGFP (C). Total lysate from each was compared by western blot. B, To evaluate the tissue expression of Nmnat2, lysate from various tissues were analyzed by western blot. Note that a slightly slower migrating band (*) is observed in several tissues including brain; this band is nonspecific as shown in *panel C*. C, Comparison of brain lysate from mice in which both *Nmnat2* alleles have been trapped (Tr/Tr) versus wild-type controls (+/+). Each lane represents a single animal. As expected (see text), Nmnat2 expression in gene trap mouse brain is ~50 % of wild-type controls. Note the same non-specific band observed in *panel B*, marked with (*). D, To evaluate the cellular expression of Nmnat2, lysates from various cell types were analyzed by western blot. Nmnat2 is detected in a human neuroblastoma cell line SH-SY5Y, but not in primary glia, U87 or U343—which are glioblastoma cell lines—or either of the negative controls: NIH3T3 or HEK293T. In SH-SY5Y, Nmnat2 is dramatically upregulated upon differentiation. E, Nmnat2

expression increases during maturation of primary cortical neurons similarly to Syb 2, a critical synaptic vesicle protein. F, Expression of Nmnat2 during mouse development; mouse brain lysate was obtained from a pair of male and female mice at birth and every 4 d thereafter as indicated. For each panel, an equal amount of protein was loaded in each lane; actin, GAPDH or VCP are used as loading controls. (*) indicates non-specific band.

control). Total lysate from N2a was analyzed by western blot and a band migrating at the expected molecular weight (34.4 kDa) is observed in cells infected with control virus, but is undetectable in cells infected with shRNA targeted against *Nmnat2* (FIGURE 2.1A).

Existing studies show that Nmnat2 transcript is enriched in the brain relative to other tissues (Raffaelli et al., 2002; Sood et al., 2001; Yalowitz et al., 2004), although transcript has also been detected in heart and muscle (Yalowitz et al., 2004). To further test the specificity of this antibody, we compared lysate from various tissues and identified the same ~34 kDa band detected in FIGURE 2.1A in brain, but not heart or any other tissues examined (FIGURE 2.1B), including skeletal muscle (data not shown). Note that a slightly slower migrating band (marked with an *asterisk*) is observed in several tissues including brain suggesting that this is a nonspecific band. To determine if this band is nonspecific, we compared brain lysate derived from mice in which both *Nmnat2* alleles have been trapped. The intensity of the same ~34 kDa band observed in FIGURE 2.1A and B is reduced ~50 % (FIGURE 2.1C), consistent with a 50 % reduction in mRNA expression ($P = 0.002$, $N = 3$), while the intensity of the same slower migrating band observed in FIGURE 2.1B (*asterisk*) remains constant. This mouse line was created to analyze the physiological function of Nmnat2. A more detailed analysis of these mice will be provided in future studies. Gene traps often produce null mutants (Abuin et al.,

2007), however reduced (or even normal) expression of the underlying gene is not uncommon (Voss et al., 1998a, b).

Using western blot analysis, these data show that an antibody targeted against full-length Nmnat2 detects a band migrating at the expected molecular weight in lysate derived from brain and a neuroblastoma cell line. This band is sensitive to targeted knockdown using either shRNA or a gene-trap insertion. The intensity of this band compared to known amounts of purified recombinant Nmnat2 indicates that the abundance of endogenous protein in the brain is very low (~0.001 % of total protein). To the best of our knowledge, this is the first antibody validated to detect endogenous Nmnat2.

Based on its specific expression in the brain, we speculated that Nmnat2 may be further restricted to specific cell types, i.e. neurons or glia. Therefore we analyzed total lysate from several different cells, including SH-SY5Y, a human neuroblastoma cell line; U87 and U343, which are glioblastoma cell lines; as well as primary cultures. Nmnat2 is expressed in two neuroblastoma cell lines: SH-SY5Y (FIGURE 2.1D) and N2a (FIGURE 2.1A), and primary cortical neurons (FIGURE 2.1E), but is undetectable in primary glia or either of the glioblastoma cell lines tested (FIGURE 2.1D), suggesting that Nmnat2 is more strongly expressed in neurons.

Interestingly, Nmnat2 protein levels increase dramatically upon differentiation of SH-SY5Y (FIGURE 2.1D) and during maturation of primary neuronal cultures (FIGURE 2.1E). This effect was also observed *in vivo*, as Nmnat2 levels in the brain are relatively low at birth, and then peak toward the end of the postnatal period (FIGURE 2.1F). This expression profile is similar to Rab5, which regulates endocytosis and early endosome

fusion (Stenmark, 2009), and synaptobrevin 2 (Syb 2), which is a neuronal protein critical for normal synaptic function (Schoch et al., 2001). In contrast, neurofilament (NF, heavy chain) increases dramatically at the end of postnatal development (Shaw and Weber, 1982), while valosin-containing protein (VCP)—a chaperone (Wang et al., 2004)—remains steady throughout.

Nmnat2 Is a Palmitoylated Peripheral Membrane Protein

Nmnat2 has previously been reported to localize to the Golgi complex in HeLa cells (Berger et al., 2005). Since it is not predicted to contain a signal sequence or transmembrane domain (or lipid binding domain), we speculated that Nmnat2 localization to this organelle results from peripheral attachment via protein-protein interaction or lipid modification.

Nmnat1, -2 and -3 consist of a conserved bipartite Rossman fold linked together by a unique stretch of amino acids in the middle of the primary sequence. In addition to being poorly conserved between isoforms, this low homology domain (LHD) contains the nuclear localization sequence for Nmnat1 (Schweiger et al., 2001). To identify residues in LHD(Nmnat2) that may be required for Golgi localization, we generated several short deletion mutants (FIGURE 2.2A) and compared their localization relative to GM130, a well-characterized Golgi marker (Nakamura et al., 1995). We used lentiviruses for gene delivery to reduce potential artifacts due to high-level expression resulting from transient transfection. The localization pattern of LHD-Δ2 closely resembles full-length Nmnat2,

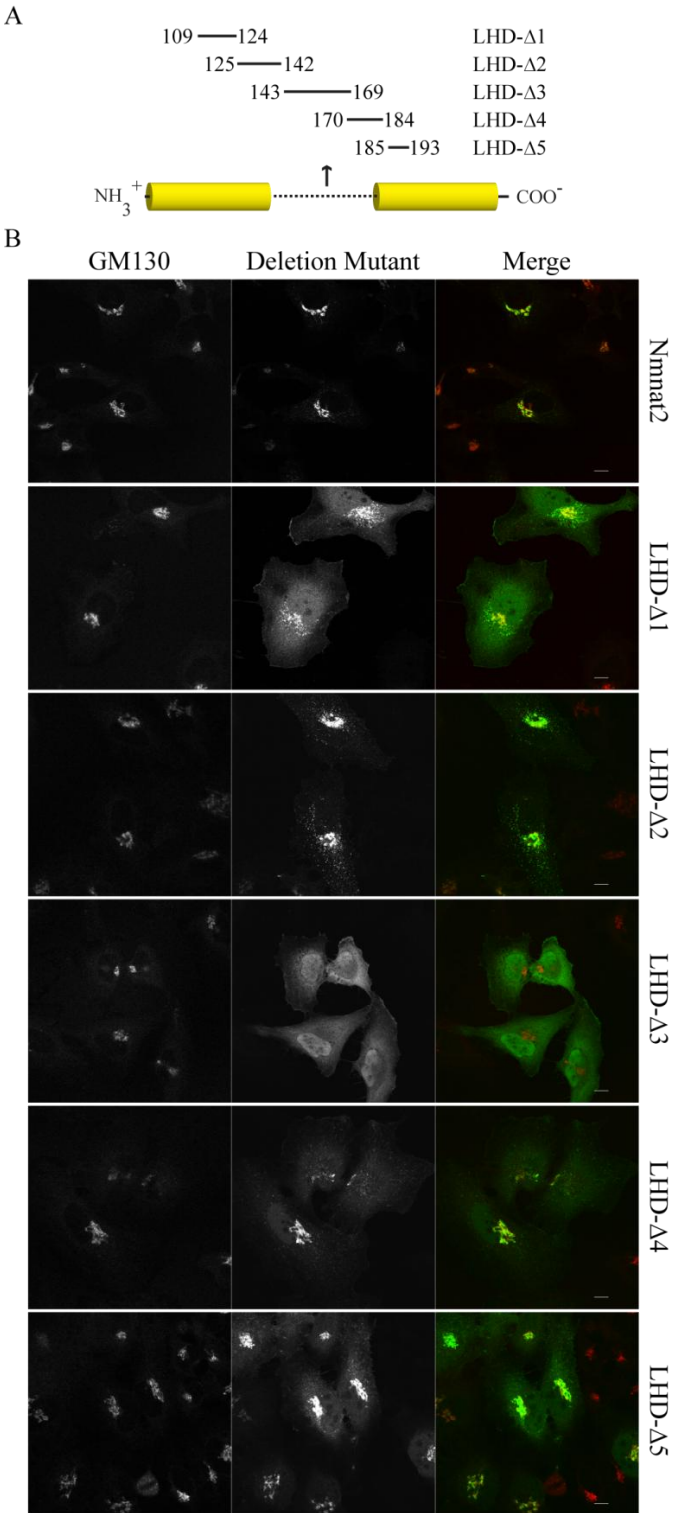
A
109—124
125—142
143—169
170—184
185—193
LHD-Δ1
LHD-Δ2
LHD-Δ3
LHD-Δ4
LHD-Δ5
NH3+
COO-
B
GM130
Deletion Mutant
Merge
Nmnat2
LHD-Δ1
LHD-Δ2
LHD-Δ3
LHD-Δ4
LHD-Δ5

FIGURE 2.2 Residues 143-169 Are Necessary for Golgi Localization and Membrane Association. A, Cartoon of human Nmnat2 (NP_055854) indicates residues that have been deleted in a given mutant. A characteristic stretch of residues poorly conserved between Nmnat1, -2 and -3, referred to as the low homology domain (LHD), is illustrated with a dotted line; conserved regions are in solid yellow. B, HeLa cells infected with lentiviruses (MOI ~3) expressing either Nmnat2 or the indicated mutant (with EGFP tag) and were fixed then probed for GM130 to assess Golgi localization. Scale bar = 10 μm..

while LHD-Δ1, LHD-Δ4 and LHD-Δ5 retain Golgi localization but have increased cytoplasmic signal (FIGURE 2.2B). This suggests that residues 109-124 (LHD-Δ1) and 170-193 (LHD-Δ4 and -Δ5) may contribute but are not required for Golgi localization. In contrast, LHD-Δ3 does not colocalize with GM130 and shows diffuse cytoplasmic localization.

Among the residues deleted in the LHD-Δ3 mutant (aa143-169), we focused on C164 and C165 given that [1] they are within a highly conserved cluster (FIGURE 2.3A) and [2] cysteines are targets of prenylation and palmitoylation (Resh, 2006). Since prenylation occurs on C-terminal CAAX motifs, we directly investigated the possibility that Nmnat2 is palmitoylated using metabolic labeling. Nmnat2, but not Nmnat2 C164S/C165S, labels with [^{3}H]-palmitate indicating that: [1] Nmnat2 is palmitoylated and [2] C164 and C165 are required for this modification (FIGURE 2.3B).

To determine if palmitoylation is required for Golgi localization, we compared the localization of Nmnat2 C164S/C165S relative to GM130. In contrast to wild-type control, but identical to LHD-Δ3 (see FIGURE 2.2B), Nmnat2 C164S/C165S appears diffuse in the cytoplasm and does not colocalize with GM130 (FIGURE 2.3C). This suggests that Nmnat2 C164S/C165S is soluble. To investigate this possibility, infected cells were treated prior

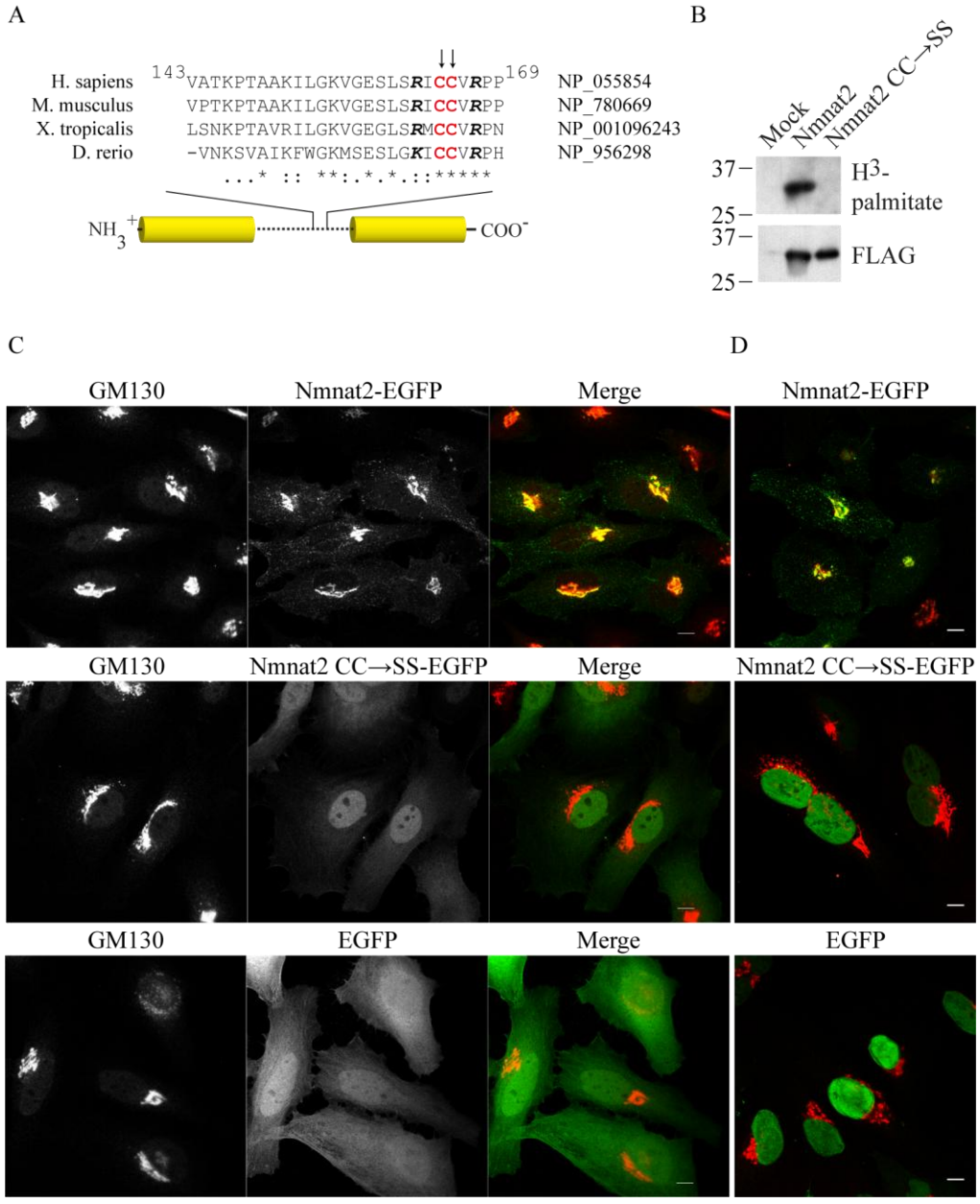

FIGURE 2.3 Nmnat2 Is a Palmitoylated Peripheral Membrane Protein. A, Sequence alignment reveals C164 and C165 as potential targets of palmitoylation. Palmitoylation lacks a well-defined motif but occurs on cysteines frequently with nearby basic residues. C164 and C165 are highlighted in red, while nearby conserved basic residues are in bold italics. B, HEK293T were transfected and metabolically labeled with [^{3}H]-palmitate. Following immunoprecipitation, incorporation of radiolabel was assessed by in-gel fluorography. To assess the efficiency of immunoprecipitation, a 1:10 dilution of eluted protein was analyzed by western blot (WB). C, HeLa were infected with lentiviruses (MOI = 3) expressing either

Nmnat2-EGFP, Nmnat2 C164S/C165S-EGFP or EGFP, then fixed and probed for GM130, a well-characterized *cis*-Golgi marker (Nakamura et al., 1995). D, Infected HeLa cells were permeabilized with digitonin prior to fixation to assess the solubility of wild-type Nmnat2 and C164S/C165S mutant. Note that under these conditions the nuclear membrane remains intact. Scale bar = 10 μm.

to fixation with digitonin—a mild detergent that selectively permeabilizes the plasma membrane—allowing soluble components of the cytoplasm to rapidly diffuse out of the cell. Under these conditions, cytoplasmic Nmnat2 C164S/C165S and EGFP are washed out, while wild-type Nmnat2 is retained in the cell (FIGURE 2.3D).

Although C164 and C165 are likely targets of palmitoylation, these residues could be necessary for Nmnat2 to acquire and/or maintain its tertiary structure. To test this possibility, we compared the activities of purified recombinant Nmnat2 C164S/C165S to wild-type (in parentheses): k_{cat} = 7.21 ± 0.46 s^{-1} (0.654 ± 0.50 s^{-1}), K_M^{ATP} = 112.88 ± 0.14 μM (84.25 ± 0.13 μM) and K_M^{NMN} = 2.95 ± 0.40 μM (6.91 ± 1.31 μM). Although it is unclear why Nmnat2 C164S/C165S has a faster turnover rate (k_{cat}), the mutant is fully active indicating that it is able to maintain its tertiary structure.

Consistent with membrane localization, most *endogenous* Nmnat2 sediments with a crude membrane fraction (P100) after subcellular fractionation of mouse brains in the absence of detergent (FIGURE 2.4A). To clarify its interaction with the P100 fraction, we attempted to extract Nmnat2 using a selection of reagents commonly used to solubilize peripheral membrane proteins. VCP is a chaperone that is attached to membranes via protein-protein interaction (Wang et al., 2004) and is readily soluble in 4 M urea (FIGURE 2.4B). Conversely, Rab5—a small GTPase tethered to membranes via geranylgeranylation (Kinsella and Maltese, 1991, 1992)—and synaptotagmin I (Syt I)—an integral membrane protein (Perin et al., 1990)—and Nmnat2 remain in the pellet

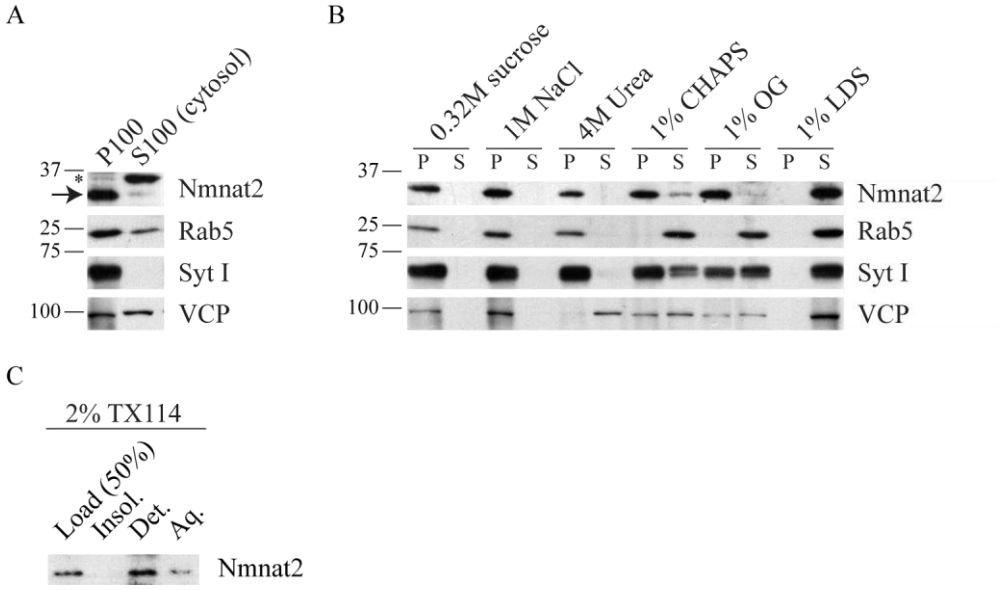

FIGURE 2.4 Biochemical Characterization of Nmnat2 Membrane Association. A, Mouse brains were homogenized and fractionated in detergent-free buffer as described in Methods section. (*) indicates non-specific band. B, To characterize the nature of the interaction between Nmnat2 and the membrane, P100 pellets were extracted with either high salt (1 M NaCl), a chemical denaturant (4 M urea), or a selection of detergents: 1 % CHAPS (zwitterionic), 1 % octyl glucoside (non-ionic) or 1 % LDS (anionic). (P) and (S) refer to pellet and supernatant collected after a 30 min extraction on ice and a subsequent 100,000 x *g* spin. C, Nmnat2 is efficiently extracted in 2 % Triton X-114 and partitions with detergent following phase separation, as expected for a palmitoylated protein.

fraction. Rab5 is readily soluble in all detergents tested, while Nmnat2, VCP and Syt I are partially soluble in CHAPS and octyl glucoside. This is expected for VCP since these detergents lack the necessary polarity to efficiently disrupt protein binding. Similarly, Syt I also binds numerous proteins at the membrane which probably accounts for its partial solubility under these conditions. Because endogenous Nmnat2 is resistant to extraction with 4 M urea, but slightly soluble in CHAPS and octyl glucoside, this suggests that: [1] palmitoylation recruits Nmnat2 to detergent resistant membranes or [2] Nmnat2 is tightly held at the membrane via protein binding and palmitoylation.

Finally, we assessed the behavior of *endogenous* Nmnat2 in a solution of Triton X-114. Triton X-114 has a similar structure to Triton X-100 but is more hydrophobic and has a lower cloud point. At temperatures above the cloud point, a detergent solution spontaneously separates into aqueous and detergent phases. Because Triton X-114 is a non-denaturing detergent, proteins with hydrophobic surfaces—such as transmembrane and lipid-modified proteins—partition with the detergent phase, while hydrophilic proteins remain in the aqueous phase (Bordier, 1981). In contrast to its solubility in Triton X-100 (data not shown) Nmnat2 is readily soluble in the more hydrophobic Triton X-114, and it is highly enriched in the detergent phase following phase separation (FIGURE 2.4C).

In summary, Nmnat2 localization to the Golgi requires palmitoylation, while mutation of C164 and C165 to serine abolishes this modification and results in a soluble, active protein. Furthermore, despite its lack of a transmembrane domain (or lipid-binding domain) *endogenous* Nmnat2 has the biochemical characteristics of a membrane protein. Taken together, these data strongly suggest that Nmnat2 is peripherally anchored to membranes via palmitoylation.

Sufficiency of Nmnat2 Low Homology Domain (LHD) for Golgi Localization

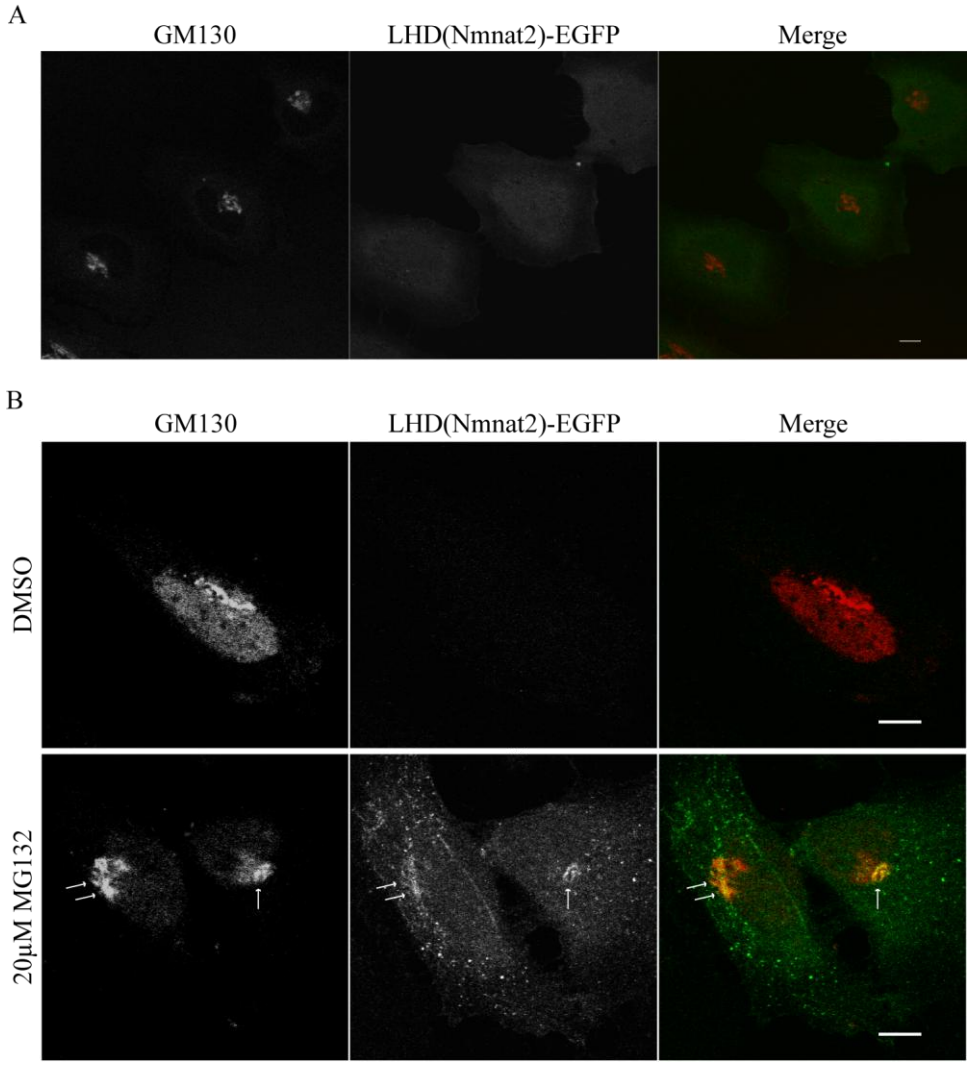

FIGURE 2.5 Nmnat2 Low Homology Domain Is Insufficient for Stable Interaction with Golgi. A, HeLa infected with lentivirus (MOI ~3) expressing LHD(Nmnat2)-EGFP were fixed and probed for GM130. B, Treatment of these cells with a proteosome inhibitor, MG132 (20 μM, 2.5 h), boosts the overall intensity of fluorescent signal revealing weak colocalization between LHD(Nmnat2)-EGFP and GM130 (*arrows*). Images were taken using the same exposure settings for both DMSO (negative control) and MG132 treated cells. Scale bar = 10 μm

LHD(Nmnat2) was cloned in-frame with EGFP to determine if this region is sufficient for Golgi localization. Although fluorescent signal in these cells is low, LHD(Nmnat2)-EGFP shows diffuse cytoplasmic localization (FIGURE 2.5A) similar to

Nmnat2 C164S/C165S and LHD-Δ3. Based on this observation we speculated that LHD(Nmnat2)-EGFP may be unstable. Following treatment with MG132, a proteosome inhibitor, LHD(Nmnat2)-EGFP weakly colocalizes with GM130 (FIGURE 2.5B). This suggests that residues outside the low homology domain are required for stable interaction of Nmnat2 with Golgi.

Overexpression of Nmnat2 Is Toxic to Primary Neurons

Although the antibody described here is useful for detection of endogenous Nmnat2 by immunoblotting, it is unsuitable for immunohistochemistry experiments due to unacceptably high background. All commercially available Nmnat2 antibodies, as well as several other in-house antibodies were also tested but with similar results (data not shown).

To assess the localization of Nmnat2 in neurons, primary cultures were infected with lentivirus expressing either Nmnat2 or Nmnat2 C164S/C165S. Unexpectedly, overexpression of wild-type Nmnat2 is toxic to neurons resulting in pervasive cell death (FIGURE 2.6A). In contrast, Nmnat2 C164S/C165S is well tolerated, indicating that increased NMN adenylyltransferase activity alone is not sufficient for toxicity. Furthermore, toxicity is not observed in non-neuronal cells (e.g. HeLa) and is independent of affinity tags (data not shown). This suggests that the levels of endogenous Nmnat2 must be tightly regulated and may account for its low abundance. Nonetheless, prior to the onset of toxicity, exogenous Nmnat2 localizes to Golgi—consistent with its reported localization in HeLa (Berger et al., 2005)—as well as vesicles in dendrites and axons (FIGURE 2.6B).

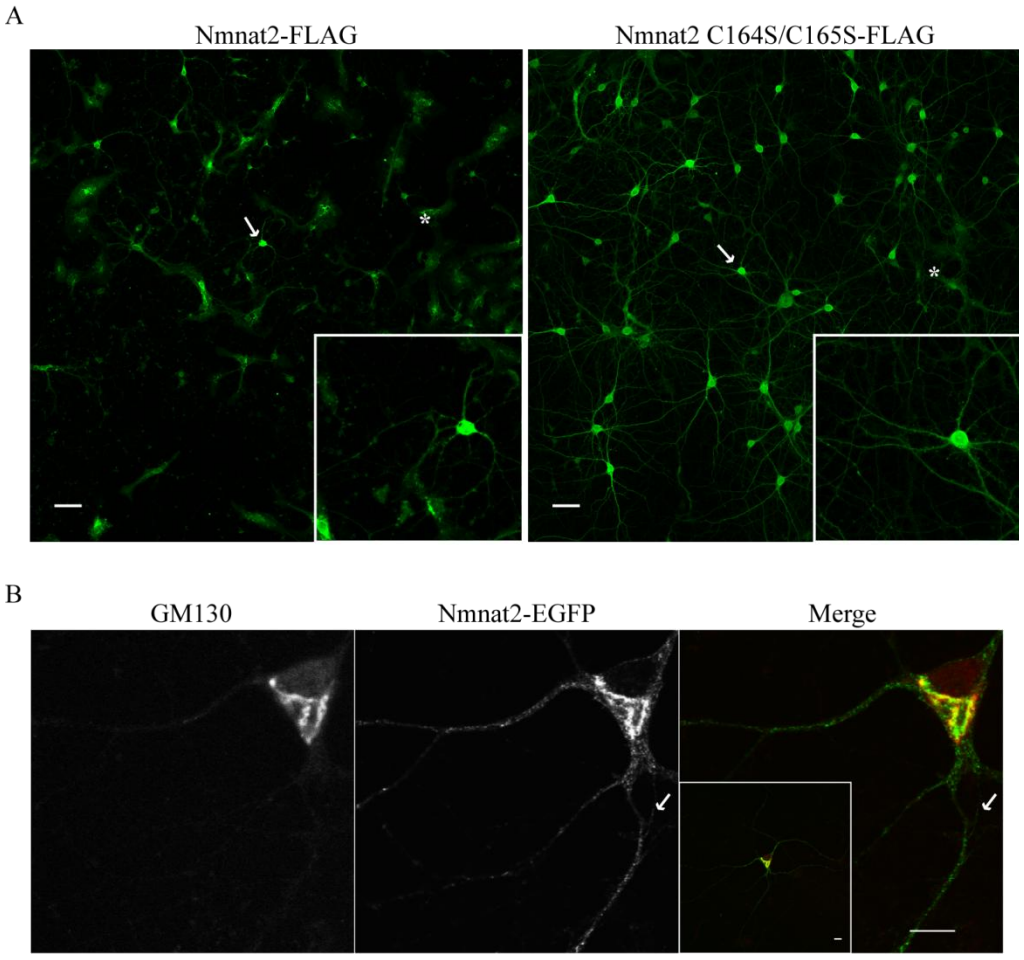

FIGURE 2.6 Exogenous Nmnat2 Is Toxic to Primary Neurons. **A,** Primary cortical neurons were infected with lentivirus expressing either Nmnat2-FLAG or Nmnat2 C164S/C165S-FLAG. ~4 d after infection, cultures were fixed and probed with an anti-FLAG antibody. Nmnat2, but not Nmnat2 C164S/C165S, is toxic to neurons resulting in massive neuronal death; arrows indicate neurons shown in inset. For comparsion, a glia cell in each image is marked with (*). Scale bar = 50 μm. B, Primary cortical neurons were infected with lentivirus (MOI ~3) expressing Nmnat2-EGFP. Nmnat2 localizes to Golgi (as in HeLa cells) but also dendrites and axons (scale bar = 10 μm); magnified view of a dendrite (*lower panel*, scale bar = 2 μm).

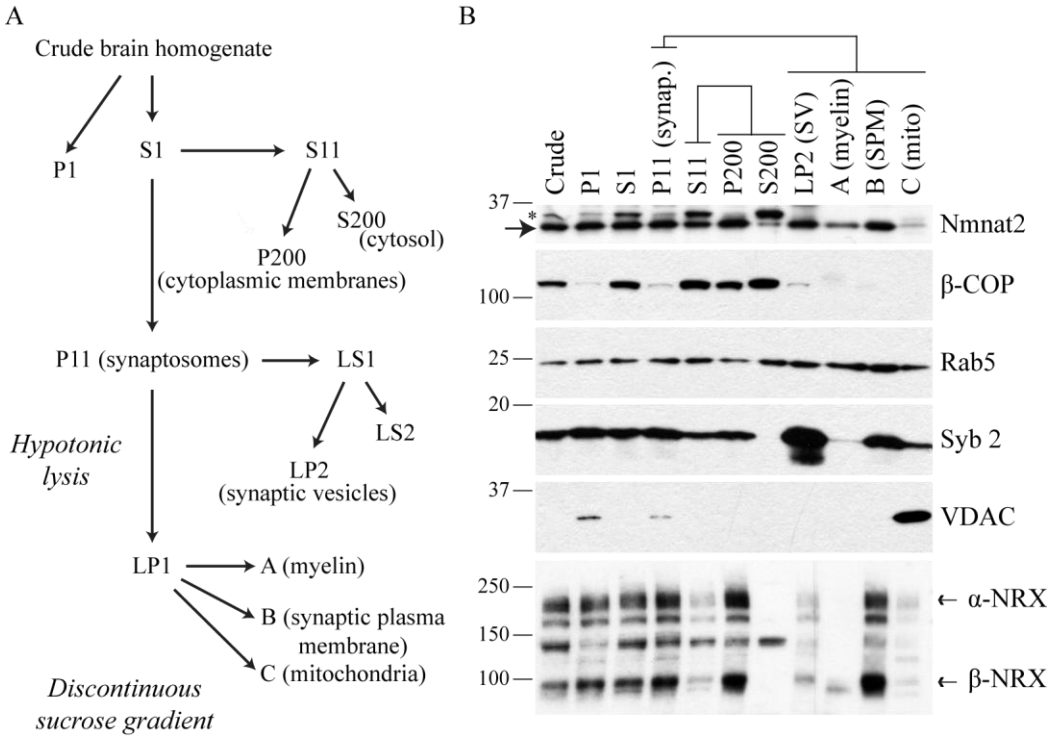

FIGURE 2.7 Endogenous Nmnat2 Localizes to Synaptic Terminals. A, Schematic of synaptosome purification protocol. Synaptosomes are detached nerve terminals formed during homogenization and contain membranes derived from both pre- and post-synaptic compartments. For P1, S1, P11, S11, P200 and S200; P refers to pellet and S refers to supernatant, while numbers refer to the force of centrifugation for each step (e.g. S200 = supernatant resulting from 200,000 x *g* spin). B, Western blot analysis of fractionated mouse brains; an equal amount of protein was loaded for each sample. (*) indicates non-specific band.

Nmnat2 Localizes to Synaptic Terminals (i.e. Synaptosomes)

Palmitoylation is a common mechanism used by neurons to sort peripheral membrane proteins to specific compartments including axons, dendrites and synapses (El-Husseini Ael et al., 2001; Huang and El-Husseini, 2005; Kang et al., 2008). To determine if endogenous Nmnat2 localizes to any of these structures, mouse brain synaptosomes—which are detached nerve terminals formed during homogenization (Whittaker, 1993)—were purified and fractionated yielding pellets enriched for synaptic

vesicles, myelin, synaptic plasma membrane and mitochondria (see FIGURE 2.7A for schematic).

Nmnat2 is enriched equally between synaptosome (P11) and cytoplasmic membrane (P200) enriched fractions, unlike β-COP, which in neurons is found exclusively in the cell body (Sannerud et al., 2006) and is highly enriched in P200 and cytosol (S200) (FIGURE 2.7B). β-COP is a coatmer protein that continually cycles on/off transport vesicles between the *cis*-Golgi and ER (Duden, 2003; Duden et al., 1991; Griffiths et al., 1995; Oprins et al., 1993). In contrast to β-COP, Rab5 localizes to both pre- and post-synaptic terminals (de Hoop et al., 1994; Fischer von Mollard et al., 1994) and is detected in all fractions. Further purification of synaptosomes (P11) shows that Nmnat2 co-purifies with markers for synaptic vesicles (synaptobrevin 2) (Takamori et al., 2006) and synaptic plasma membrane (α/β-neurexins) (Butz et al., 1999). Note that α/β-neurexins (NRX) only minimally contaminate LP2 (synaptic vesicle enriched fraction), suggesting that this fraction is relatively free of plasma membrane. Since Nmnat2 is not detected at the plasma membrane when overexpressed (see FIGURES 3C, *top panel* and 6B), its co-purification with α/β-NRX in fraction B may indicate the presence of dendrite-derived endosomes—consistent with the presence of Rab5 in this fraction as well. Taken together with our observation that Nmnat2-EGFP localizes to vesicles in dendrites and axons (FIGURE 2.6B), these data suggest that endogenous Nmnat2 localizes to vesicles in synaptic terminals.

Nmnat2 Localizes to Rab7-Containing Late Endosomes and Trans-Golgi Network in HeLa Cells

Under normal growth conditions, when overexpressed at low levels via lentiviral infection (MOI = 3), Nmnat2 localizes not only to Golgi but also to cytoplasmic vesicles (e.g. FIGURES 3C, *top panel* and 6B). Localization is independent of the presence of an affinity tag (data not shown). A subset of these structures colocalize with Rab7 (FIGURE 2.8), a late endosome marker (Feng et al., 1995). In some instances Nmnat2 and Rab7 are adjacent or only partially co-localize. Nmnat2 also colocalizes with perinuclear TGN46, a *trans*-Golgi network (TGN) marker (Ponnambalam et al., 1996). In contrast, there is no significant overlap with EEA1, an early endosome marker (Mu et al., 1995), indicating that Nmnat2 localizes to specific compartments in the endosomal pathway. Consistent with its presence at synaptic terminals, these results suggest that Nmnat2 is transported to these compartments via an endosomal pathway.

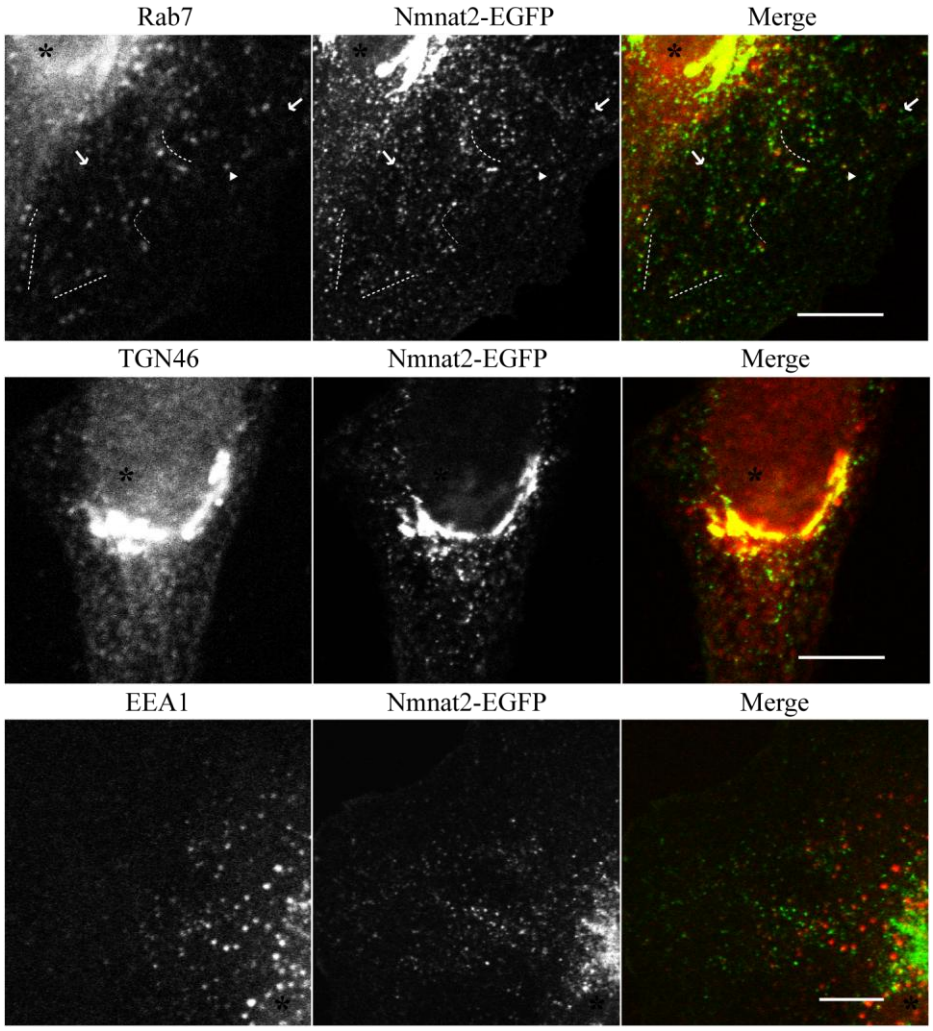

FIGURE 2.8 Nmnat2 Localizes to Rab7 Late Endosomes and *Trans*-Golgi Network in HeLa Cells. HeLa were infected with lentiviruses (MOI = 3) expressing Nmnat2-EGFP, then fixed and probed for Rab7, a late endosome marker (Feng et al., 2000) (*top panel*); TGN46, a *trans*-Golgi network marker (Ponnambalam et al., 1996) (*middle panel*); or EEA1, an early endosome marker (Mu et al., 1995) (*bottom panel*). Dotted lines indicate regions in the cytoplasm where Rab7 and Nmnat2 are closely associated. Arrows indicate where Nmnat2 does not co-localize with Rab7. Arrowhead indicates specific vesicle where Nmnat2 colocalizes with Rab7. (*) marks nucleus in each cell. Scale bar = 10 μm.

Discussion

In this report, we have analyzed the expression and localization of Nmnat2 and characterized its interaction with cellular membranes. To analyze Nmnat2 protein expression, we generated and validated a polyclonal antibody against full-length protein. Out of all antibodies tested, including in-house and all commercially available antibodies, the antibody described here had the best specificity and sensitivity. Nmnat2 is detected exclusively in neurons with expression peaking shortly after birth suggesting that these cells require additional NAD synthesis during early postnatal development. Although this coincides with an intense period of synaptogenesis (Knaus et al., 1986), the reason for an increase in expression during this time remains to be determined.

Overexpression of Nmnat1, -2 or -3 in neurons has been demonstrated to slow the rate of axon degeneration *in vivo* and *in vitro* (Beirowski et al., 2009; Conforti et al., 2009; Press and Milbrandt, 2008; Sasaki et al., 2006; Yan et al., 2009). Although the underlying mechanism remains to be elucidated, axon degeneration precedes neuronal cell body death in many neurodegenerative diseases including Alzheimer's and Parkinson's suggesting that manipulation of NAD synthesis pathways may provide new therapeutic targets (Raff et al., 2002).

Paradoxically, overexpression of Nmnat2 is toxic to primary neurons (but not other cell types such as HeLa), while Nmnat2 C164S/C165S is well tolerated, indicating that excess Nmnat activity alone is insufficient to cause toxicity. One possible explanation for this phenotype is that exogenous Nmnat2, but not Nmnat2 C164S/C165S, forms aggregates that are toxic to neurons (but not other cell types). However, this scenario is unlikely given the highly reducing environment of the cytoplasm.

Alternatively, exogenous Nmnat2 may form a spurious interaction with one or more proteins at the membrane. It has recently been suggested that such interactions are a common cause of toxicity resulting from protein overexpression (Vavouri et al., 2009). The lack of gross toxicity in non-neuronal cells may therefore be due to the absence (or low abundance) of a specific interacting protein. Another possibility is that exogenous Nmnat2 in neurons binds to a *bona fide* protein target, but toxicity results from overstimulation of an existing metabolic or signaling pathway.

Using superior cervical ganglia cultures, Gilley and Coleman have recently shown that *endogenous* Nmnat2 localizes to axons and that Nmnat2-EGFP particles are transported via fast axonal transport (Gilley and Coleman, 2010). Here we show prominent localization of Nmnat2-EGFP to dendrites and axons; and that *endogenous* Nmnat2 localizes to synaptic terminals. Consistent with our observation, Zhai et al. report that *Drosophila* Nmnat localizes to synaptic puncta (Zhai et al., 2006) suggesting a conserved function for Nmnat at synapses.

While this paper was being reviewed, Lau et al. published an analysis of the low homology domain (LHD) of Nmnat1, -2 and -3 (which they refer to as isoform-specific targeting and interaction domains—i.e. ISTID1, ISTID2 and ISTID3) (Lau et al., 2010). These authors report that Nmnat2 is palmitoylated on C164 and C165. We also show that Nmnat2 is palmitoylated but conclude *only* that C164 and C165 are required for this modification. Furthermore we report that *endogenous* Nmnat2 has the biochemical characteristics of a membrane protein despite lacking a transmembrane domain or lipid binding domain; and Nmnat2 is difficult to solubilize, suggesting that it is either: [1] recruited to detergent resistant membranes or [2] tightly held at the membrane via protein

binding and palmitoylation. Additionally, Lau et al. report that expression of FLAG-ISTID2-EGFP, consisting of residues 108-190, is sufficient for Golgi localization. In contrast, we find that LHD(Nmnat2)—defined as residues 109-193—is *insufficient* to stably interact with Golgi membranes. Future experiments will investigate the effect of the low homology domain on overall stability of Nmnat2.

It remains to be determined what specific role Nmnat2 plays in neuronal NAD metabolism, and specifically, what advantages its localization and membrane association provide. However, the data presented here provide a solid foundation from which these questions can better be addressed.

Attributions and Publications

The data presented in this chapter has been published (Mayer et al., 2010). All of the experiments in this chapter were conceived, designed and executed by me with the exception of the kinetic characterization of Nmnat2 and Nmnat2 C164S/C165S, which was done by Nian Huang, a postdoctoral researcher in Hong Zhang's lab (UTSW). On occasion, Colleen Dewey provided me with primary neurons. Dan Dries provided significant editorial assistance with the resulting manuscript.

CHAPTER THREE:

PRODUCTION AND ANALYSIS OF *NMNAT2* GENE TRAP MICE

Abstract

Its unique localization and brain-specific expression prompted us to generate *Nmnat2* null-mutant mice to investigate its physiological function. Toward this end we established two gene trap mouse lines using commercially available ES cells. Our initial characterization of these mice revealed incomplete trapping of *Nmnat2* in both lines resulting in ~50% reduction of Nmnat2 protein expression in homozygotes. These mice appear normal and histological analysis of brain sections provides no indication of neurological pathology.

Introduction

To investigate the physiological function of Nmnat2, we relied on a gene trap based approach using ES cells obtained from BayGenomics. Each mouse line was derived from a unique clone and named accordingly: RRF238 and YHC280. The trap used to generate the ES cells, pGT0lxf, contains a β-galactosidase/neomycin (β-geo) reporter flanked by the *engrailed-2* splice acceptor (SA) and the SV40 poly-adenylation (pA) signal. Because it lacks a promoter, this trap is designed to insert into the coding sequence of an active gene and terminate transcription following recognition of the

polyadenylation signal (Abuin et al., 2007). Gene traps often result in null mutants. However reduced (or even normal) expression of the underlying gene is not uncommon (Voss et al., 1998a, b).

Pellagra is a disease caused by insufficient dietary uptake of NAD precursors. In humans, it is characterized by the 4 D's: diarrhea, dermatitis, dementia and death (Hegyi et al., 2004). Since Nmnat catalyzes the final step in NAD biosynthesis and Nmnat2 is highly enriched in the brain, we speculated that a null mutant mouse may mimic the neurological pathology observed in Pellagra patients.

Here we report that in two different mouse lines *Nmnat2* is trapped, albeit inefficiently, resulting in ~50% reduction in protein expression. Histological analysis of brain sections obtained from mice homozygous for trap reveals no clear signs of neurological pathology commonly associated with pellagra. Finally, neither line is useful for expression analysis using the β-gal reporter due to unknown reasons. Although gene trap technology may be useful for large scale screens, investigators interested in a specific target are cautioned to consider the potential caveats of this approach.

Methodology

Generation of Nmnat2 Gene Trap Mice

RRF238 and YHC280 ES cells were obtained from BayGenomics for a nominal fee. These cells were generated using the pGT0lxf trap (see Introduction for a description). Rapid amplification of 5′ cDNA ends (5′-RACE) located pGT0lxf in the first intron of mouse *Nmnat2* for both cell lines (this information was provided by

BayGenomics). Note that for YHC280 the International Gene Trap Consortium database indicates that pGT0lxf is located within the first exon. However, manual analysis of the sequence data provided does not support this conclusion suggesting that this is an artifact of automated processing. Injection of ES cells into C57Bl/6 blastocysts was performed in-house at the UTSW Transgenic Technology core facility. Chimeric male mice (F0) were breed to wild-type C57Bl/6 females and their progeny (F1) were screened for germline transmission by PCR. Heterozygous breeding pairs were setup with males and females from different litters but within the same line. The progeny of these matings (F2) were used for the experiments described here.

Genotyping (RRF238 colony)

The location of the RRF238 trap was determined by iterative touchdown PCR using nested primer pairs consisting of a specific forward primer which anneals at the 3′ end of pGT0lxf and hemi-degenerate reverse primer, essentially as described (Guo and Xiong, 2006). To help distinguish candidate bands from background noise, genomic DNA from separate mice with the same genotype was used as template for adjacent PCR reactions. After two rounds, a single band was selected for DNA sequencing from RRF238 template. This fragment contained the junction between pGT0lxf and genomic DNA revealing that in the RRF238 line the trap inserted immediately upstream of 154769018bp on chromosome 1 in the first intron of *Nmnat2*. The location of pGT0lxf in the YHC280 line could not be determined using this or any other approach tested.

Instead, these mice were genotyped by quantifying pGT0lxf copy number as described below.

For the RRF238 colony, mice were genotyped by PCR using following parameters: 10min/93C initial incubation; then 40 cycles of 30s/93C, 45s/60C, 90s/65C and followed by a final extension step of 10min/65C.

TABLE 3.1 Primers for Genotyping RRF238 Mice:

#	Primer:	Sequence:	Tm	Product	Conc.
236	238F_1	cttgggagccaatgtgggg	59.7	359bp	400nM
237	238R_1	aggaagcagggagaggcag	59.8	-	500nM
238	238TrapF_1	TGCAAGGCGATTAAGTTGGGTAACG	60	206bp	500nM

Quantitative RT-PCR

RNA from adult mouse brains was purified using TRIzol reagent (Invitrogen), reverse-transcribed from random primers using SuperScript II (Invitrogen) and quantified by PCR using SYBR FastGreen PCR Master Mix (Applied Biosystems) according the manufacturer's instructions. Primers were designed to generate PCR products that crossed the junction between exons 1 and 2 (see below). All reactions were performed in triplicate on an Applied Biosystems 7500 Real-Time PCR System. Statistical analysis was performed using SigmaPlot 11 (Systat Software).

TABLE 3.2 Primers for *Nmnat2* (mouse) qRT-PCR:

Gene	Gene ID	Primer #	Sequence
Cyclophilin	NM_011149	CS	ggagatggcacaggaggaa
		CS	gcccgtagtgcttcagctt
qN2e1-2/(1)	NM_175460	307	CCACAAAGACCCACGTTATCCT

	308	CCCTGGCTCTCTCGAACATC

Endpoint RT-PCR

RNA from adult mouse brains was purified using TRIzol reagent (Invitrogen) and reverse-transcribed from random primers using SuperScript II (Invitrogen) according the manufacturer's instructions.

TABLE 3.3 Primers for Endpoint RT-PCR:

#	Primer:	Sequence:	Tm	Product
246	mGAPDHe3_F	TTCCAGGAGCGAGACCCCa	60.8	246bp
247	mGAPDHe4_R	GCTAAGCAGTTGGTGGTGCAG	59.7	
260	mN2e1_F(2)	CAAAGACCCACGTTATCCTGCTGg	60.5	308bp
269	mN2e4_R	CTTCATCAGGTCTCGATGGTGCT	59.1	
260		same as above		330bp
261	mN2betaGeo_R1	gcgccattcgccattcagg	60.7	

Quantitative PCR for Genotyping (YHC280)

For accurate and reproducible results it is essential to use high quality genomic DNA. Digest ~0.5cm piece of **ear** in 400µl SNET/Proteinase K at 55°C by shaking at 1100rpm for 4-24 h. SNET/Proteinase K is prepared as follows: 20mM Tris-HCl/pH8, 5mM Na_2EDTA, 1% SDS, 400mM NaCl; add fresh 0.5mg/ml proteinase K immediately before use. Add 400µl phenol/cholorform/isoamyl alcohol (25:24:1, v/v, Roche), mix well and spin for 10 min at 13000rpm (RT). Carefully transfer supernatant to fresh tube (~300µl), add 300µl isopropanol, shake well and precipitate DNA for 10 min on ice. It is

essential to be very careful when transferring supernatant to avoid contamination from either phenol/chloroform or tissue debris. Spin for 15 min at 13000rpm (4°C), discard supernatant. Wash pellets with 1ml 70% EtOH and spin for 5 min. Discard supernatant and carefully suction dry pellets—do not allow pellet to completely dry. Add 200µl of TE and dissolve pellet with shaking for 5-10 min (RT). To further purify samples, transfer to 100,000MWCO Microcon filter (Millipore) and centrifuge at 500 x *g* for ~10min—do not allow membrane to dry. Add 500µl of sterile nanopure quality water and centrifuge. Repeat.

pGT0lxf copy number is quantified by PCR using SYBR FastGreen PCR Master Mix (Applied Biosystems) according the manufacturer's instructions (1.25µl of template/20µl reaction volume). All reactions were performed in triplicate on an Applied Biosystems 7500 Real-Time PCR System. Statistical analysis was performed using SigmaPlot 11 (Systat Software).

TABLE 3.4 Primers for Genotyping YHC280 Mice by qPCR:

Gene	Accession	Primer #	Sequence
Delta-like 1	NM_007865	DL1/F	gtc tca gga cct tca cag tag
		DL1/R	gag caa cct tct ccg tag tag
qTrap/F and R (5)	na	323	GCCGGTCGCTACCATTACC
		324	GATTGTCTGTTGTGCCCAGTCA

Protein Expression Analysis

Brains were washed with PBS, then immediately flash-frozen in liquid nitrogen and ground to powder using a mortar and pestle. This powder was lysed with cold 50mM HEPES-NaOH, 1% LDS, 1mM DTT and protease inhibitors (0.2mM PMSF, 0.5μg/ml leupeptin and 1μM pepstatin A) and then briefly sonicated to reduce viscosity. Protein concentration was measured using the DC protein assay according to the manufacturer's instructions (Bio-Rad) and samples were analyzed by SDS-PAGE/WB. Validation of the Nmnat2 antibody used for this experiment is presented elsewhere.

Pathology

For sample preparation, mice were perfused with paraformaldehyde using standard methods. Following dissection, brains were transferred to 50ml conical tubes and allowed to continue fixing for an additional 3-4days at room temperature. The brains were then transferred to the Pathology core (UTSW) where they were sectioned, stained and analyzed.

Results

To assess the level of *Nmnat2* expression in RRF238 and YHC280 mice it was first necessary to develop a reliable genotyping strategy. Although numerous strategies are available, we chose to use a PCR-based approach given its low cost and simplicity. However gene traps insert randomly into the genome and their precise location must be

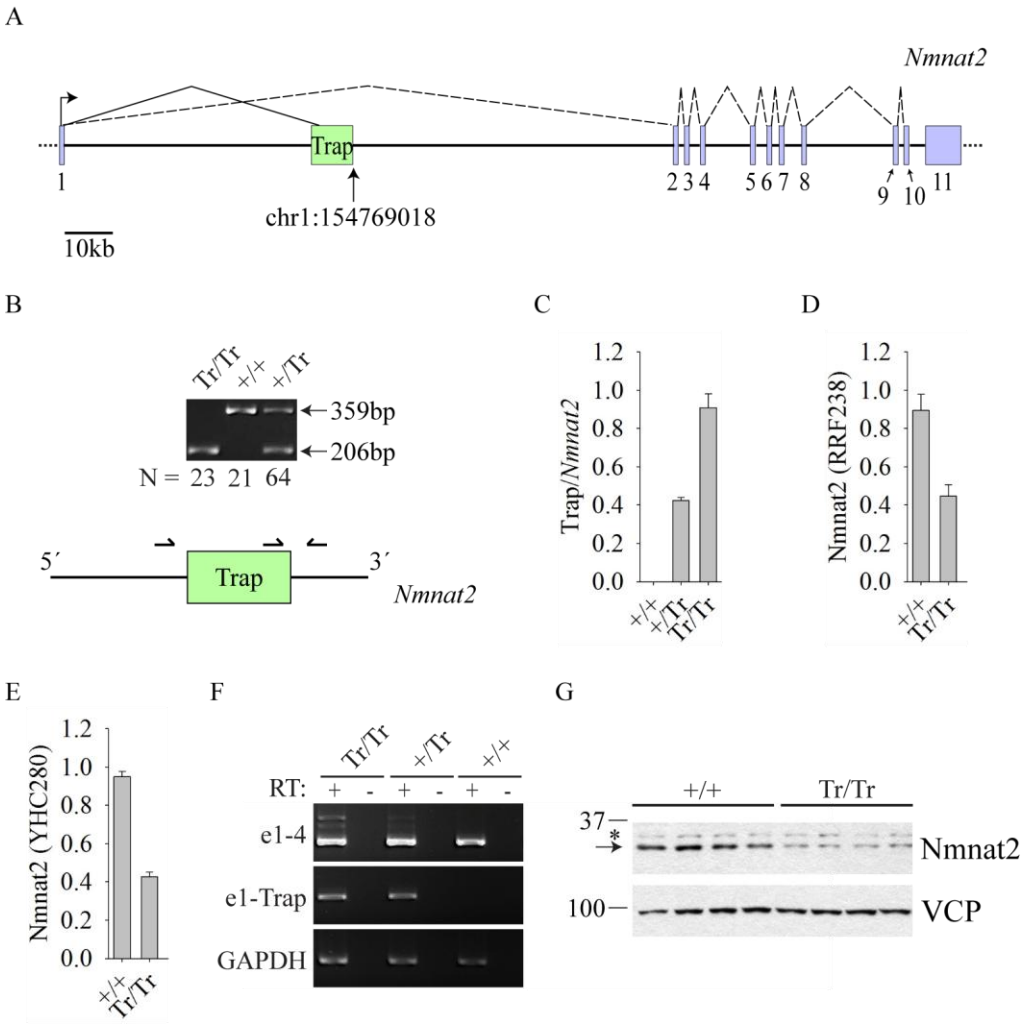

FIGURE 3.1 Partial Gene Trapping of Nmnat2 with RRF238 and YHC280 ES Cell Lines. A, Scale drawing of mouse *Nmnat2* (Gene ID: 226518). For RRF238, pGT0lxf trap is located in the first intron immediately upstream of the position indicated on chromosome 1 (154769018). Although we were unable to determine the location of pGT0lxf in the YHC280 line, these mice were genotyped by quantifying trap copy number (e.g. see *panel C*). B, For the RRF238 colony, the distribution of genotypes is approximately 1:1:2. This result is expected assuming that pGT0lxf inserted into genome at only location. C, To confirm our genotyping strategy, the trap copy number was determined using quantitative PCR (qPCR). Consistent with the assigned genotypes, there is no trap detected in wild-type control, and twice as much trap in the homozygote *versus* heterozygote (RRF238). D (RRF238) and E (YHC280), To assess the efficiency of trapping expression of *Nmnat2* mRNA levels in the brain were measured using qRT-PCR. For these experiments, primers were designed to flank the junction between exons 1 and 2. N = 3 (except for wild-type control in *panel E* where N = 1). F, End-point RT-PCR was used to determine the presence of wild-

type transcript in mouse brains (YHC280). An identical PCR product is readily detected in samples from all three genotypes using primers designed to amplify exons 1-4 (*top panel*). Splicing between exon 1 and the trap is observed in homozygous and heterozygous samples, but absent in the wild-type control. G, Western blot analysis of total protein extracted from mouse brains (RRF238). Each lane represents a separate animal; 40μg protein/lane. VCP is used as a loading control. *Asterisk* indicates non-specific band.

determined prior to primer design. For the RRF238 line this was accomplished using a genome walking strategy (data not shown), which located the trap approximately halfway through the first intron (chr1:154769018) (FIGURE 3.1A). The distribution of genotypes in this colony is roughly Mendelian (FIGURE 3.1B). Quantification of the trap copy number per *Nmnat2* allele is consistent with the assigned genotype (FIGURE 3.1C). Because we were unable to locate pGT0lxf in the YHC280 line, these mice were genotyped by this approach. Unexpectedly, quantification of *Nmnat2* mRNA in homozygous mouse brains from both colonies reveals a loss of only ~50% relative to wild-type controls (FIGURE 3.1D and E). Since these experiments used primers that flank the splice junction between exons1 and 2, this suggests that in both lines the *engrailed-2* splice acceptor is partially ignored. Consistent with this possibility, endpoint RT-PCR demonstrates the presence of wild-type transcript in a homozygous brain (FIGURE 3.1F, *top panel*). Finally, western blot analysis shows ~50% of Nmnat2 protein levels in homozygous brains relative to wild-type controls (FIGURE 3.1G). Taken together, these data show partial trapping of *Nmnat2* in two independent gene trap mouse lines.

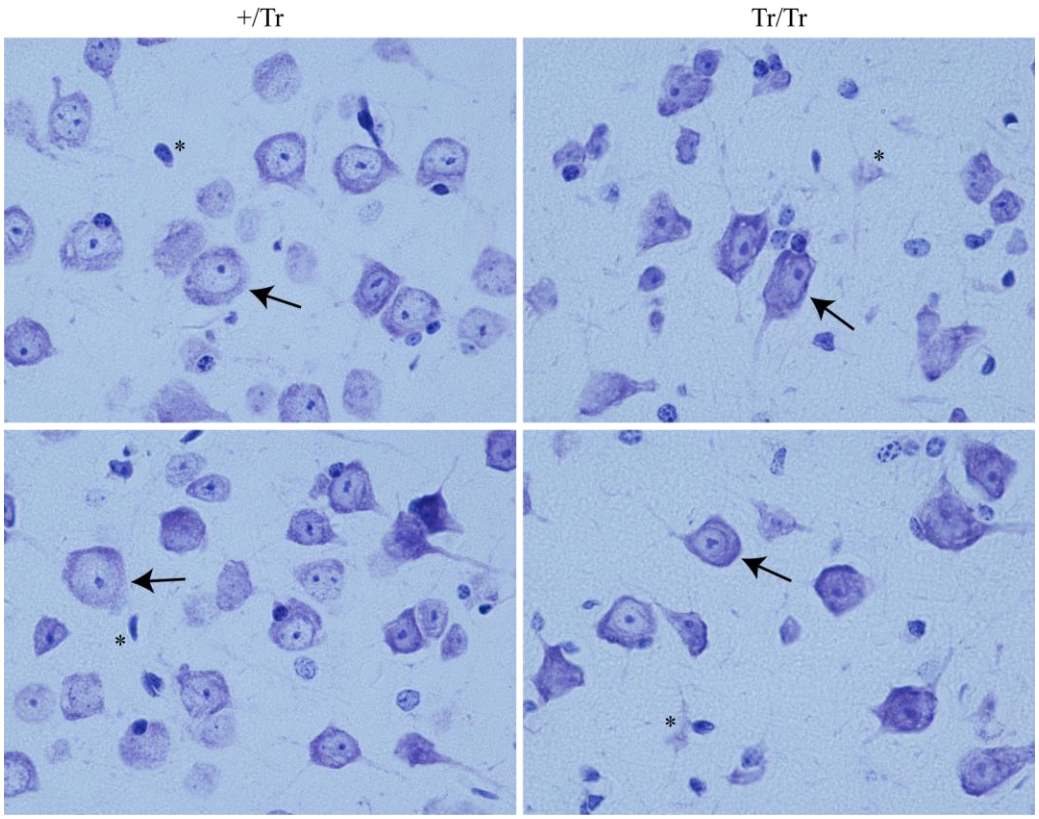

FIGURE 3.2 Histological Analysis of Brain Slices from RRF238 Colony. Representative Nissl staining of brain sections from heterozygote (+/Tr) and homozygote (Tr/Tr) brain sections. Two separate images of the lower cortex for each genotype are shown. *Arrows* denote neurons, while *asterisks* indicate any other cell type including astrocytes and oligodendrocytes.

A key pathological feature of Pellagra is chromatolysis of Betz cells and other large neurons in the cortex (Hamill, 1912; Ishii and Nishihara, 1981). Chromatolysis refers to the clearing of Nissl substance (rough ER) from the cell body of neurons—Nissl staining labels DNA and RNA, and is a classic histological technique used to analyze the health of neurons (Cragg, 1970). There are no signs of chromatolysis in brain slices from pGT0lxf homozygous mice (FIGURE 3.2). Furthermore, no signs of pathology were observed following hematoxylin and eosin (HE) staining (data not shown). Although

these mice appear normal relative to controls, homozygotes tend to be smaller (data not shown).

X-gal staining of RRF238 homozygote brains was unsuccessful for unknown reasons (data not shown)—brains from YHC280 mice were not tested. However, this is not an uncommon problem observed in gene trap mice (Voss et al., 1998b).

Discussion

It is unclear why pGT0lxf only partially traps *Nmnat2* transcript, but this observation in two independent mouse lines suggests a context dependent effect. Alternatively, the design of the pGT0lxf trap may be flawed. The lack of a clear phenotype observed in either RRF238 or YHC280 homozygotes could be due to [1] expression of residual wild-type protein, and/or [2] a subtle physiological function. Nonetheless the production of a *bona fide* null mutant will be essential to determine the specific role of Nmnat2 in brain NAD metabolism.

Attributions and Publications

All of the experiments in this chapter were conceived, designed and executed by me. This data has not been published.

CHAPTER FOUR:

CONCLUSIONS AND RECOMMENDATIONS

Introduction

The goal of this dissertation is to characterize the expression, localization, biochemistry and cellular/physiological function of Nmnat2. Although the function of Nmnat2 remains unclear, the work presented here represents a significant and original contribution to the field of NAD biology.

The essential steps for NAD biosynthesis have long since been identified (Magni et al., 1999), but the arrangement of these chemical reactions varies between cells (and organisms). Little is known about the consequences of these differences. For example, vertebrates express three Nmnat isoforms that have different kinetic properties, expression patterns and subcellular localization (Lau et al., 2009), suggesting that Nmnat1, -2 and -3 have evolved specialized roles in vertebrate NAD metabolism. I chose to focus on Nmnat2 since it is found only in the brain and Nmnat overexpression slows the rate of Wallerian degeneration.

Neuronal Localization of Nmnat2

Data presented here demonstrate that Nmnat2 is a peripheral membrane protein anchored via palmitoylation and expressed predominately in neurons.

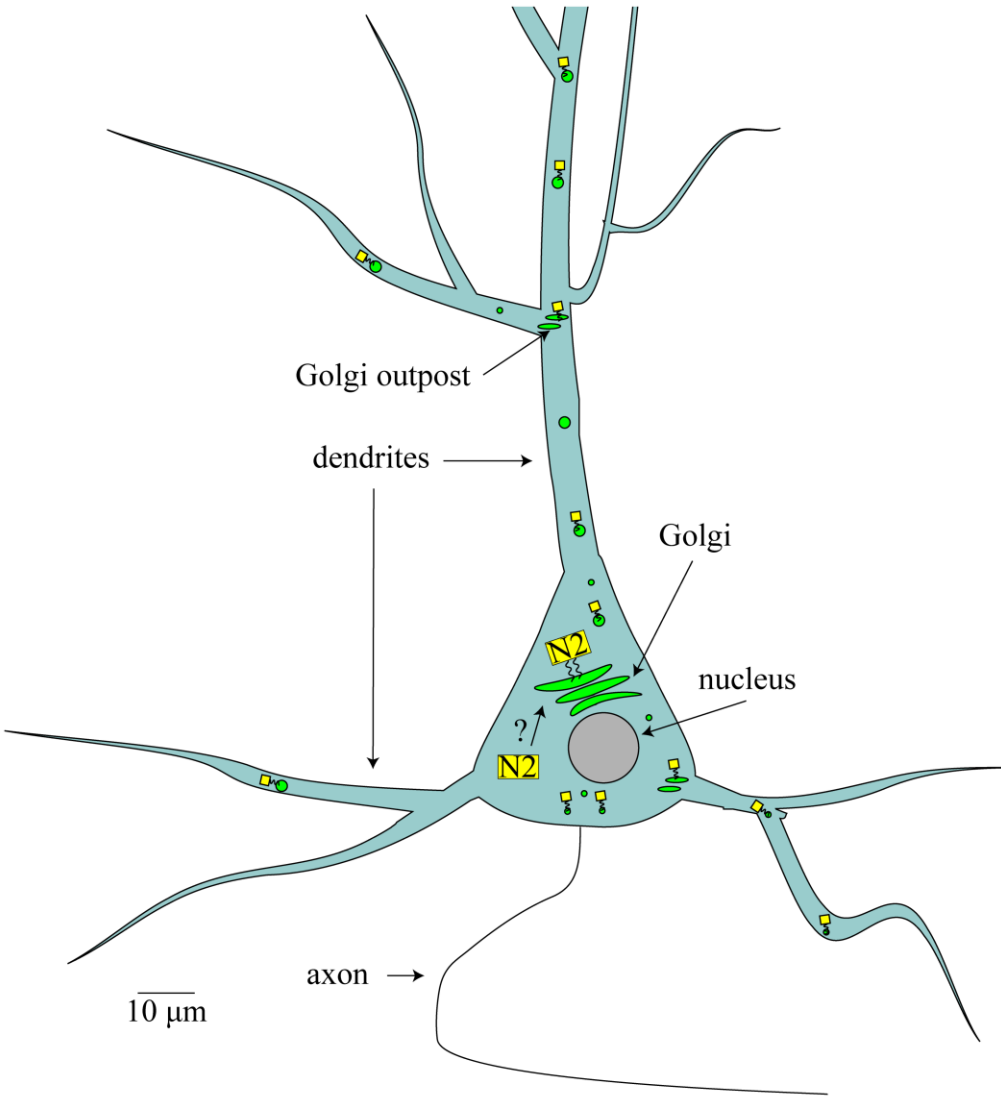

FIGURE 4.1 Localization of Nmnat2 in Neurons. Nmnat2 lacks a known signal sequence, transmembrane domain or lipid-binding domain and is peripherally attached to membranes via palmitoylation. Since palmitoylation is thought to occur exclusively on membranes (see text), it is unclear how Nmnat2 is initially recruited. Overexpression experiments indicate that Nmnat2-EGFP localizes to vesicles (green circles) in the neuronal cell body and dendrites with some signal also observed in the proximal end of the axon. These observations are consistent with biochemical data indicating that endogenous Nmnat2 co-purifies with synaptosome and cell body membrane markers. Yellow squares denote Nmnat2. This illustration depicts a simplified pyramidal neuron (scale is approximated).

Given the lack of a known signal sequence, transmembrane domain or lipid-binding domain, this strongly suggests that Nmnat2 faces the cytoplasm. Recently published data has confirmed this assumption (Lau et al., 2010). It is generally accepted that palmitoyltransferases are membrane bound and although there is some disagreement on their specific localization (Ohno et al., 2006; Rocks et al., 2010), palmitoyltransferases are often found on Golgi membranes (Noritake et al., 2009). Consistent with this observation, overexpression studies demonstrate that Nmnat2 spends at least part of its life cycle at the Golgi (Berger et al., 2005; Lau et al., 2010). Furthermore, it is shown here that exogenous Nmnat2 also traffics to Rab7-containing late endosomes in HeLa cells. Partial biochemical purification of endogenous Nmnat2 demonstrates colocalization with synaptosome membrane markers and overexpression in primary neurons, prior to the onset of toxicity, shows that Nmnat2-EGFP localizes to vesicles in dendrites and the neuronal cell body, with only a few vesicles observed in the proximal end of the axon (FIGURE 4.1).

Palmitoylation is a common post-translational modification often used by neurons to sort proteins to specific membrane compartments (El-Husseini Ael et al., 2001; Huang and El-Husseini, 2005; Kang et al., 2008). Thus, palmitoylation may exclude endogenous Nmnat2 from axons. Alternatively, the relative lack of Nmnat2 in axons can be explained by the following observations. Nmnat2 is reported to have a half-life of less than 4 h (compared to greater than 72 h for Nmnat1 and -3) (Gilley and Coleman, 2010); my unpublished observations indicate that Nmnat2 turnover is approximately 1 h. Anterograde axon transport of membrane associated proteins is approximately 8-16 mm/h (200-400 mm/d); soluble proteins and small molecules (e.g.

nucleotides) move even slower at an average rate of approximately 0.08-0.3 mm/h (2-8 mm/d) and 0.3 mm/h (6 mm/d), respectively (Lasek et al., 1984). Although there is ample evidence for local protein synthesis in dendrites, it remains unclear if local translation occurs within axons; it has been suggested that intercellular transport of glia-derived proteins can explain this phenomena (Giuditta et al., 2008). Note that I was unable to detect Nmnat2 expression in either primary glia or glioblastoma cell lines. Furthermore, Golgi and so-called Golgi outposts are found exclusively in dendrites but not axons (Horton et al., 2005). Assuming that most endogenous Nmnat2 is attached to vesicle and/or Golgi membranes, which is supported by biochemical data presented here,

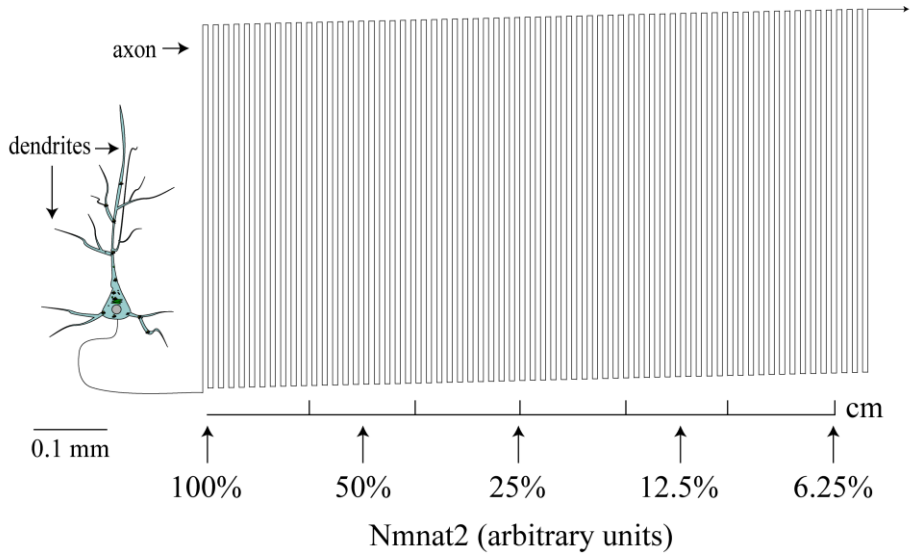

FIGURE 4.2 Nmnat2 Gradient at the Proximal End of the Axon. The rate of fast axon transport (0.8–1.6 cm/h) and the rapid turnover of Nmnat2 (~1 h) suggest that endogenous Nmnat2 is largely absent from axons. For simplicity, the axon pictured here is unbranched and only 6 cm long; *in vivo*, many axons are highly branched, which would further dilute the local concentration of Nmnat2, and some axons extend up to a meter or more. For this illustration, fast axon transport is assumed to be 1.5 cm/h. Scales are approximate.

and given that dendrites are generally much shorter than axons (which can extend up to several meters in mammals), and that fast axon transport is actually fairly slow, taken together, these data strongly suggest that endogenous Nmnat2 is located in the neuronal cell body and/or dendrites but is largely absent from axons (FIGURE 4.2).

Role of Nmnat2 in Wallerian Degeneration

Exclusion of endogenous Nmnat2 from axons is consistent with recent data showing that slow Wallerian degeneration requires Nmnat activity in the axon (Babetto et al., 2010; Sasaki and Milbrandt, 2010). This necessity for axonal Nmnat suggests that 1) when overexpressed, exogenous Nmnat1, -2 or -3 improperly localizes to axons; and 2) local consumption of NAD within a damaged axon, in the absence of the ability to synthesize more, reduces the local NAD concentration prompting an orderly sequence of self-destruction (through an unknown mechanism).

Importantly, Sasaki and Milbrandt report that the transfer of Nmnat1 to severed axons up to 2 h after transection is sufficient to dramatically slow Wallerian degeneration (Sasaki and Milbrandt, 2010). Thus the decision to initiate fast (i.e. normal) axon destruction may occur within a discrete period of time, and beyond this point, degeneration occurs through a much slower alternate pathway[1]. This may explain how

[1] It has been suggested that slow Wallerian degeneration occurs through a fundamentally different mechanism that normal axon degeneration (Beirowski et al., 2005). If correct, under normal conditions, both pathways may operate simultaneously.

exogenous Nmnat2 can initiate slow Wallerian degeneration (Feng et al., 2010; Yan et al., 2009), despite its rapid turnover[2].

It has recently been argued that Nmnat2 localizes to axons and is essential for normal axon maintenance (Gilley and Coleman, 2010). This conclusion is based primarily on immunoblotting of dissected axons from superior cervical ganglia explants[3], indicating the presence of endogenous Nmnat2, and knockdown experiments demonstrating that axons degenerate spontaneously in the absence of sufficient Nmnat2 levels. Unfortunately, these experiments provide no information regarding the distribution of Nmnat2 in the axon. Nonetheless, it is plausible that endogenous Nmnat2 forms a concentration gradient in axons (see discussion above). Consistent with this notion, the rate of degeneration is faster when axons are cut at the distal end (Lubinska, 1982).

---

[2] I have also observed that Nmnat2 overexpression delays axon degeneration, despite obvious signs of Nmnat2-dependent toxicity (unpublished observations). Although this effect is not as robust as is observed for Nmnat1, it is similar in magnitude to that observed for Nmnat3 overexpression.

[3] For these experiments, Gilley and Coleman appear to have used the 2E4 monoclonal antibody, which was generated using the carboxy-terminal of Nmnat2 (human; identical to mouse). In my hands, the 2E4 antibody was not sensitive or specific enough to detect endogenous protein (data not shown). These authors do not provide data verifying the specificity of their antibody. Presumably these authors were also unable to identify an antibody suitable for detection of endogenous protein by immunofluorescence.

It is unclear if there is a disadvantage to slow axon degeneration *in vivo*. Naturally occurring mutant mice that overexpress Nmnat1 appear normal with no overt

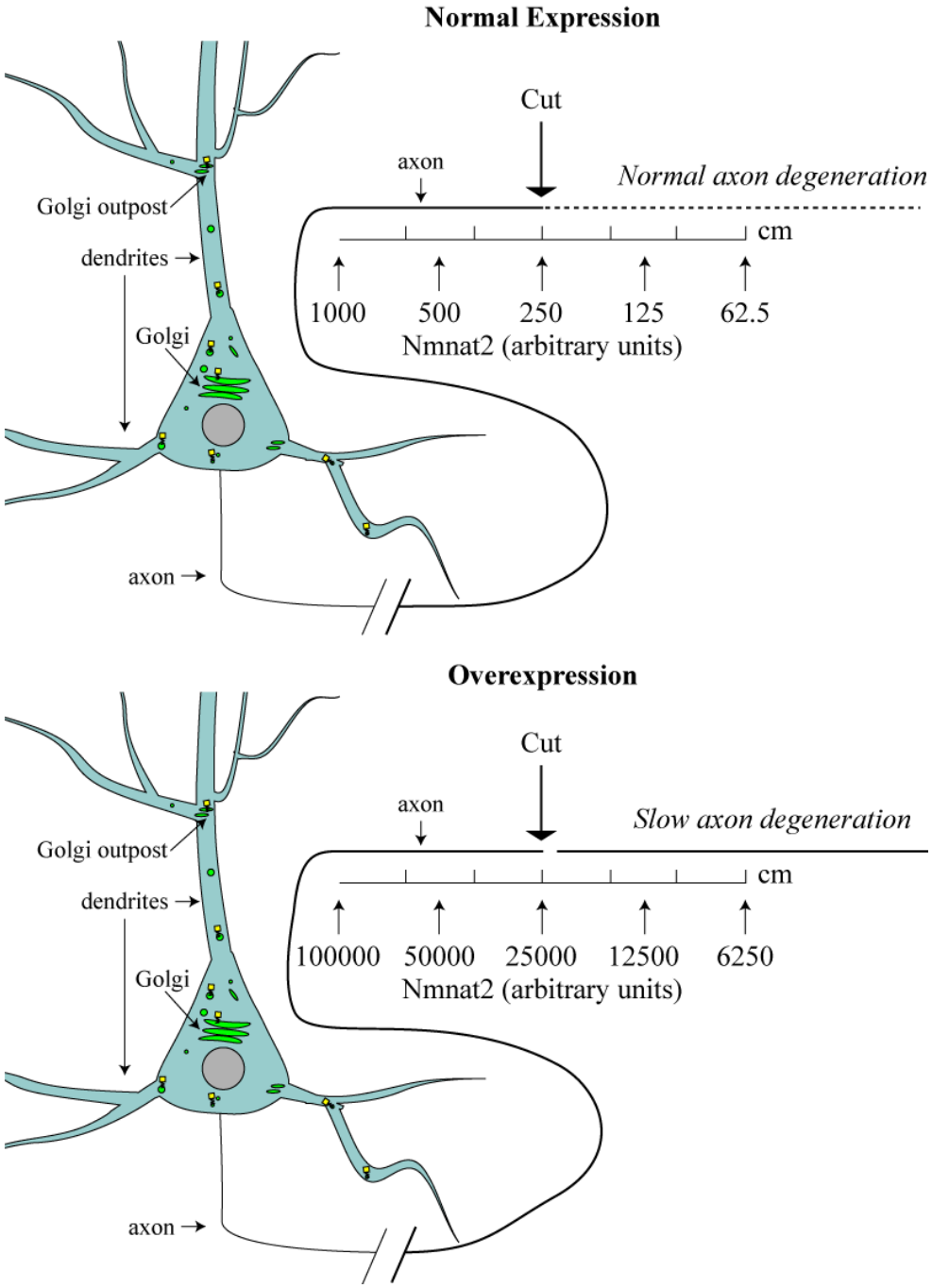

FIGURE 4.3 Model for Nmnat2 Mediated Slow Wallerian Degeneration. Neurons overexpressing

Nmnat2 display slow Wallerian degeneration *in vitro* (see text). This phenotype is also observed when neurons overexpress Nmnat1 and -3. If endogenous Nmnat2 does traffic through axons, it is likely to form a steep gradient due to the rapid Nmnat2 turnover, which may be essential for rapid clearance of damaged axons. When overexpressed, the local concentration of Nmnat2 in axons likely increases. Recent data from independent labs indicates that Nmnat activity in the axon slows degeneration. This provides a rationale for the exclusion of endogenous Nmnat2 from axons. Yellow squares denote Nmnat2.

pathology (Lunn et al., 1989; Mack et al., 2001); however, it has also been suggested that slow degeneration inhibits axon regeneration (Brown et al., 1992; Vargas and Barres, 2007). Nonetheless, if there is an advantage gained from quickly removing damaged axons, this would provide a rationale for limiting the supply of Nmnat2 in axons (FIGURE 4.3).

Possible Regulatory Function of Nmnat2

It is unknown why vertebrates express three different Nmnat isoforms. One possibility is that the subcellular location of NAD synthesis serves a regulatory function. This hypothesis makes two key assumptions: 1) most NAD is protein-bound resulting in low levels of free NAD, and 2) NAD-dependent reactions, including sirtuins (and possibly other NAD-consumers), are regulated—at least in part—by the availability of free NAD under physiological conditions. Alternatively, Nmnat1, -2 and -3 may directly bind to specific protein targets and regulate their activity via substrate channeling; however, thus far, there is little evidence to support this narrow set of conditions.

It is not currently possible to directly measure free NAD concentration within the cell, but studies on the mobility of small molecules *in vivo* (Soler-Llavina and Sabatini,

2006) support the idea that free NAD levels are much lower than the total concentration. Furthermore, a correlation between NAD concentration and sirtuin activity has been observed in numerous settings (Revollo et al., 2004; Rodgers et al., 2005; Yang et al., 2007) and it was recently shown that free NAD levels vary substantially between subcellular compartments (Dolle et al., 2010)[4]. These observations support the notion that Nmnat1, -2 and -3 serve unique regulatory functions within a given compartment.

As discussed above, palmitoylation-dependent recruitment of Nmnat2 to the membrane facilitates its localization to dendrites and the neuronal cell body. However, this localization may also allow Nmnat2 to regulate specific NAD-dependent reactions at the membrane. Consistent with this model, Nmnat1 and SIRT1 interact on the promoters of specific genes (Zhang et al., 2009). Although sirtuin regulation is complex (see Introduction), this data suggests that under certain conditions Nmnat1 may directly regulate SIRT1 activity by increasing the local concentration of free NAD or substrate channeling (it is unclear if Nmnat1 directly binds SIRT1).

Biochemical characterization of endogenous Nmnat2 indicates that it is difficult to solubilize suggesting that it may be held at the membrane via protein-protein interaction in addition to palmitoylation; or alternatively, palmitoylation may recruit Nmnat2 to detergent resistant membranes. Initial experiments using overexpressed FLAG-tagged Nmnat2 and immunoprecipitation combined with mass spectrometry did not reveal any promising candidate interactions. Nonetheless, the half-life of NAD *in vivo* is approximately 10 h, which is much longer than the half-life of Nmnat2 (see

[4] These authors measured free NAD by analyzing poly-ADP-ribose formation after expression of a compartment specific poly-ADP-ribose polymerase reporter construct.

above) indicating that Nmnat2 is an ideal candidate for regulating local NAD concentrations.

Nmnat2-Dependent Neuronal Cell Death

It is unclear why Nmnat2 overexpression causes cell death in primary cultured neurons but not other cell types (e.g. HeLa, primary glia). Since Nmnat2 C164S/C165S appears to be well-tolerated in neurons, this could be due to aggregation resulting from spurious disulfide bonds. However, in general, it is unclear if aggregation *per se* is toxic or protective (Kaganovich et al., 2008; Lansbury and Lashuel, 2006) and it has recently been suggested that toxicity resulting from overexpression is frequently caused by spurious protein-protein interaction (Vavouri et al., 2009). Alternatively, if Nmnat2 has a regulatory function, high-level expression may over-activate target pathways resulting in toxicity. Finally, localization of Nmnat2 to axons may itself be toxic.

Summary and Future Directions

Although the cellular and physiological function of Nmnat2 remains unclear, the data presented here provide a solid foundation on which to answer these questions. Although future efforts would undoubtedly benefit from access to a highly specific and sensitive antibody capable of detecting endogenous Nmnat2 by immunofluorescence or an Nmnat2-null mutant mouse, there are many interesting questions that do not require these tools and could yield important clues regarding the function of Nmnat2: identifying the mechanism of Nmnat2-dependent neuronal cell death, identifying potential Nmnat2-

protein interactions, analyzing the effect of the low homology domain on Nmnat2 turnover and activity, and solving the 3D-structure of Nmnat2.

Nmnat2 has been a difficult protein to study. However, a flurry of recent papers on Nmnat2 indicates that there is growing recognition of its potential importance. NAD is an ancient and ubiquitous small molecule. It is not surprising that enzymes have evolved multiple uses for NAD. In light of its importance and multiple functions, it is also not surprising that NAD biosynthesis is complex and likely to be compartmentalized. It will be fascinating to not only learn the precise role of Nmnat2 in neuronal biology, but to figure out how, or even if, Nmnat2 function overlaps with Nmnat1 and Nmnat3.

CHAPTER FIVE:

SUPPLEMENTAL DATA

Nmnat Overexpression Slows Wallerian Degeneration: *In vitro* axon degeneration assay using DRG explants

Overexpression of Nmnat1, -2 or 3 in neurons slows the rate of axon degeneration *in vitro* (Press and Milbrandt, 2008; Sasaki et al., 2006; Yan et al., 2009). Presented here is a protocol and representative data from preliminary experiments that is consistent with existing data indicating that Nmnat activity is necessary and sufficient for slow Wallerian degeneration phenotype. At the time this project was started, only Nmnat1 overexpression had been shown to slow Wallerian degeneration. It was not yet known if Nmnat2 or Nmnat3 overexpression would have similar effect. Subsequently, however, data has been published by others indicating that this is the case (Press and Milbrandt, 2008; Yan et al., 2009).

Axon Degeneration Assay; Dorsal Root Ganglia (DRG) Explants

The purpose of this protocol is to culture DRG explants dissected from E13 mouse embryos.

Materials:

1. DM (store at 4°C)- 500ml
    a. 500ml Hanks (Invitrogen: with phenol red, but no Ca^{2+} or Mg^{2+})
    b. 5ml HEPES (1M, Sigma: for TC, see CMD)

   c. 5ml Pen/Strep (100X , lab stock)
2. DMK
   a. Prepare day of dissection, store on ice- 100ml
   b. 50ml DM; use (2)-50ml conicals
      i. 1:1000 kainic acid (-20°C)
      ii. DNase (from CMD stock, concentration and source not known)
3. NB27Q+/-NGF
   a. Prepare ahead of time, store at 4°C
      i. 500ml Neurobasal media (Invitrogen)
         1. B-27 (Invitrogen); 10ml from stock
         2. 2mM glutamine; 5ml from 100X stock
   b. Add 1ml B-27 and 50µl of NGF stocks to 50ml "working" media

Procedure:

Preparation of glass bottom dishes (Mat-Tek, P35GC-1.5-14-C)

1. Wash glass with ~200ml 1N HCl for 15min (RT)
2. Aspirate, then wash with copious amount of PBS and repeat

Coat with PDL/Matrigel

1. Add ~100µl of 0.1mg/ml PDL (Borate buffer)
2. Incubate for ~1h/RT
3. Aspirate, then wash with copious amount of ddH_2O and repeat
4. Allow to dry under TC hood (at least 2h)
5. Add ~100µl of Matrigel (1:100, diluted in HBSS) and incubate at RT for 2h
6. Aspirate, then add minimal amount of media (just enough to fill well)

Explant DRG- direct plating

1. Add ~200µl of NB27Q+NGF (100ng/ml) to each well, store in incubator until ready
2. Perform dissection under TC hood and plate DRGs in groups of 5
3. Use fine forceps to place each DRG on glass
4. Incubate overnight at 37°C with low volume (**ensure incubator has plenty of water**)

Feeding and Infection Schedule (Morning)

1. DIV1: Add 1ml media + 4μM FDU/DU
2. DIV2: Remove 0.5ml, add virus as appropriate
3. DIV3: Aspirate media (leave enough to cover well) and replace with fresh NB27Q+NGF (100ng/ml)
4. DIV6: Aspirate/replace; **cut axons**
5. DIV9: Aspirate/replace, if necessary

Axon Degeneration Assay; Axon Cutting

The purpose of this protocol is to cut axons from DRG explants and measure the rate of degeneration.

Materials:

1. Zeiss Stemi stereomicroscope:
    a. Setup in TC hood, raise sash
    b. Must be lit from below, so use (2) microtube racks to lift microscope ~2.7 cm (one up front, one in the back)
    c. Remove black cover from bottom of microscope stand
    d. Feed fiber optic cable underneath microscope and point at ~45° angle through opening, toward the back of hood
    e. Cover hole with square of glass (15cm x 15cm), kept in drawer in Johnson lab TC room
    f. Place 2cm x 2cm square of Sylgard in the center of glass (handle with care to keep it clean)
2. Micro blade holder (FST, #10053-13) and blades (FST, #10050-00); FST blades are best
3. 45°-angle Dumont forceps
4. 50ml conical with PBS

Procedure:

1. Process samples in groups, change gloves between each group to minimize potential contamination
2. Remove lid and cut by bring the blade straight down onto sample:
    a. Cut out cell body mass to include DRGs that have fallen away from main explant
    b. Make 3-4 cuts as necessary

   c. If axon bed is accidentally pulled-up then cut this away too (unless minor, judgment call)
3. Use 45°-angle forceps to remove explant and discard in PBS
4. 20 samples require about 1h to process
5. After cutting, take images of axon bed approximately 1.5-3mm away from where explant was located:
   a. Take at least 10 images of well separated axons at 20X magnification
   b. Record the time for each sample (use "DRG Imaging Form")
6. Image axon bed at 24, 48 and 72h after cutting, as indicated above

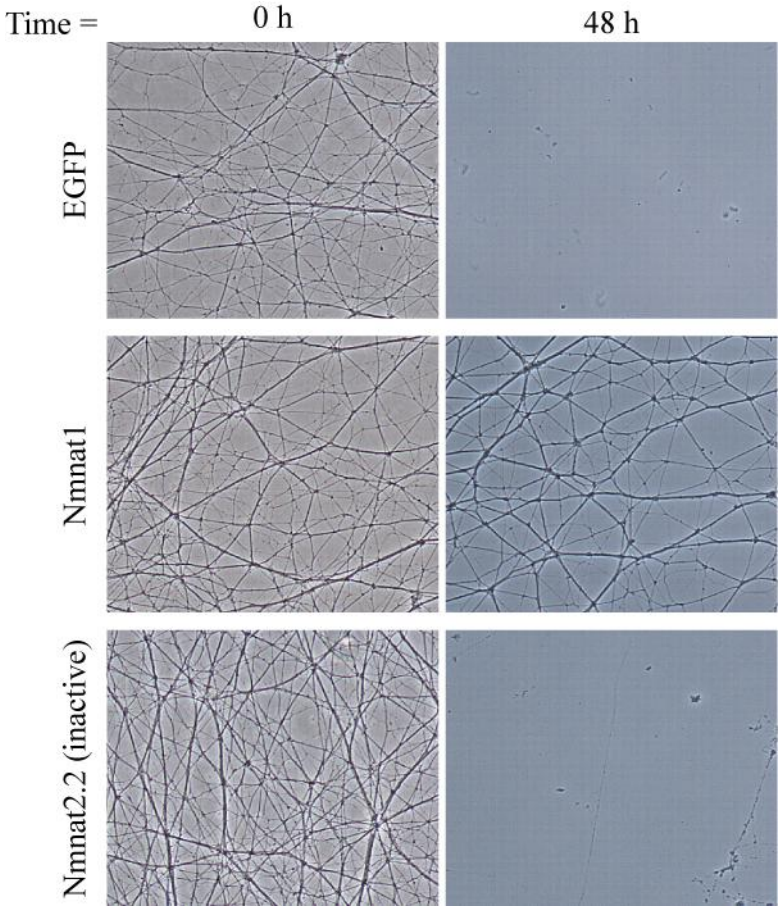

FIGURE 5.1 Slow Wallerian Degeneration Requires Nmnat Activity. Nmnat1 overexpression but not Nmnat2.2, which is a catalytically inactive splice variant of Nmnat2, slows the rate of axon degeneration following transection. Axons cut 6 days after lentivirus infection.

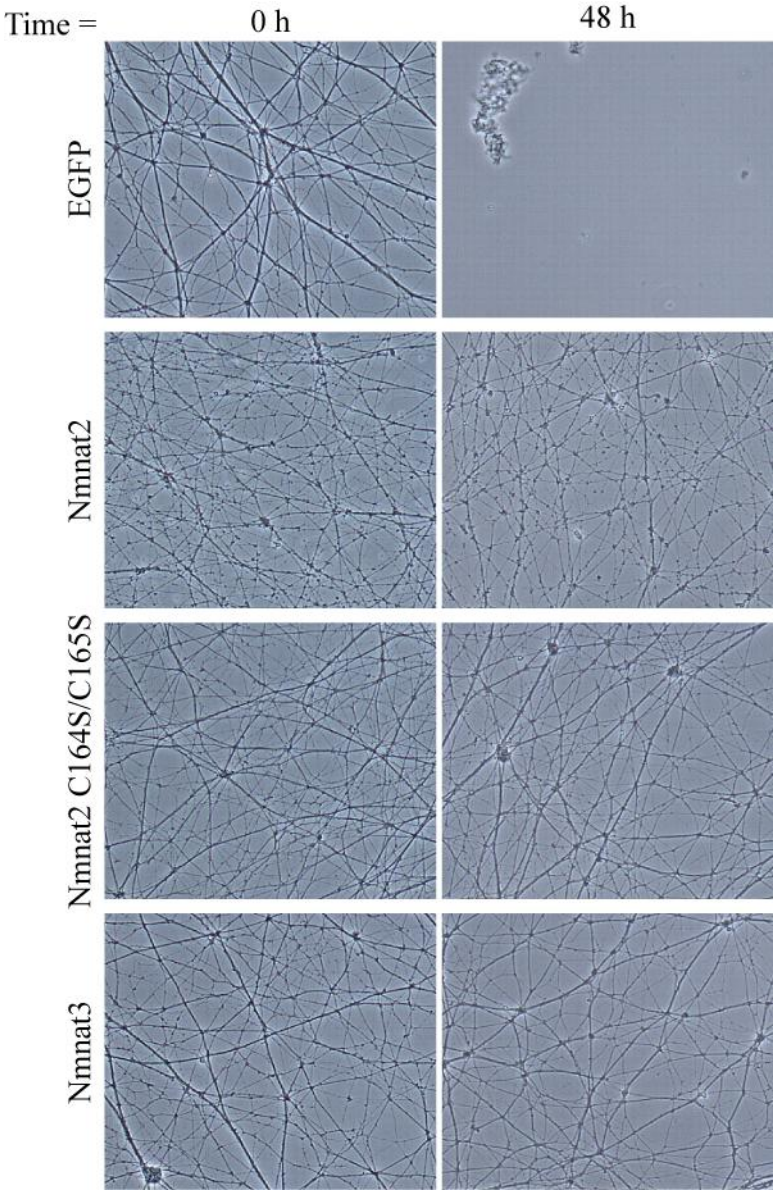

FIGURE 5.2 Nmnat2 and Nmnat3 Overexpression Slows the Rate of Axon Degeneration. Nmnat2, Nmnat2 C164S/C165S and Nmnat3 overexpression slows the rate of Wallerian degeneration in DRG explants following transection. Axons were cut 6 days after lentivirus infection. Note the "knotted" appearance of axons in cultures infected with Nmnat2. Although less pronounced than in cortical neurons, Nmnat2 overexpression is also toxic to DRG explants. Time after transection is indicated.

REFERENCES

Abuin, A., Hansen, G.M., and Zambrowicz, B. (2007). Gene trap mutagenesis. Handb Exp Pharmacol, 129-147.

Babetto, E., Beirowski, B., Janeckova, L., Brown, R., Gilley, J., Thomson, D., Ribchester, R.R., and Coleman, M.P. (2010). Targeting NMNAT1 to axons and synapses transforms its neuroprotective potency in vivo. J Neurosci *30*, 13291-13304.

Beirowski, B., Adalbert, R., Wagner, D., Grumme, D.S., Addicks, K., Ribchester, R.R., and Coleman, M.P. (2005). The progressive nature of Wallerian degeneration in wild-type and slow Wallerian degeneration (WldS) nerves. BMC Neurosci *6*, 6.

Beirowski, B., Babetto, E., Gilley, J., Mazzola, F., Conforti, L., Janeckova, L., Magni, G., Ribchester, R.R., and Coleman, M.P. (2009). Non-nuclear Wld(S) determines its neuroprotective efficacy for axons and synapses in vivo. J Neurosci *29*, 653-668.

Belenky, P., Bogan, K.L., and Brenner, C. (2007). NAD+ metabolism in health and disease. Trends Biochem Sci *32*, 12-19.

Berger, F., Lau, C., Dahlmann, M., and Ziegler, M. (2005). Subcellular compartmentation and differential catalytic properties of the three human nicotinamide mononucleotide adenylyltransferase isoforms. J Biol Chem *280*, 36334-36341.

Berger, N.A. (1985). Poly(ADP-ribose) in the cellular response to DNA damage. Radiat Res *101*, 4-15.

Bieganowski, P., and Brenner, C. (2004). Discoveries of nicotinamide riboside as a nutrient and conserved NRK genes establish a Preiss-Handler independent route to NAD+ in fungi and humans. Cell *117*, 495-502.

Billington, R.A., Travelli, C., Ercolano, E., Galli, U., Roman, C.B., Grolla, A.A., Canonico, P.L., Condorelli, F., and Genazzani, A.A. (2008). Characterization of NAD uptake in mammalian cells. J Biol Chem *283*, 6367-6374.

Bogan, K.L., and Brenner, C. (2008). Nicotinic acid, nicotinamide, and nicotinamide riboside: a molecular evaluation of NAD+ precursor vitamins in human nutrition. Annu Rev Nutr *28*, 115-130.

Bonner, W.M., and Laskey, R.A. (1974). A film detection method for tritium-labelled proteins and nucleic acids in polyacrylamide gels. Eur J Biochem *46*, 83-88.

Bordier, C. (1981). Phase separation of integral membrane proteins in Triton X-114 solution. J Biol Chem *256*, 1604-1607.

Brown, M.C., Lunn, E.R., and Perry, V.H. (1992). Consequences of slow Wallerian degeneration for regenerating motor and sensory axons. J Neurobiol *23*, 521-536.

Brusca, J.S., and Radolf, J.D. (1994). Isolation of integral membrane proteins by phase partitioning with Triton X-114. Methods Enzymol *228*, 182-193.

Butz, S., Fernandez-Chacon, R., Schmitz, F., Jahn, R., and Sudhof, T.C. (1999). The subcellular localizations of atypical synaptotagmins III and VI. Synaptotagmin III is enriched in synapses and synaptic plasma membranes but not in synaptic vesicles. J Biol Chem *274*, 18290-18296.

Ceni, C., Pochon, N., Villaz, M., Muller-Steffner, H., Schuber, F., Baratier, J., De Waard, M., Ronjat, M., and Moutin, M.J. (2006). The CD38-independent ADP-ribosyl cyclase from mouse brain synaptosomes: a comparative study of neonate and adult brain. Biochem J *395*, 417-426.

Choudhary, C., Kumar, C., Gnad, F., Nielsen, M.L., Rehman, M., Walther, T.C., Olsen, J.V., and Mann, M. (2009). Lysine acetylation targets protein complexes and co-regulates major cellular functions. Science *325*, 834-840.

Coleman, M.P., Conforti, L., Buckmaster, E.A., Tarlton, A., Ewing, R.M., Brown, M.C., Lyon, M.F., and Perry, V.H. (1998). An 85-kb tandem triplication in the slow Wallerian degeneration (Wld(s)) mouse. Proceedings Of The National Academy Of Sciences Of The United States Of America *95*, 9985-9990.

Conforti, L., Tarlton, A., Mack, T.G.A., Mi, W.Q., Buckmaster, E.A., Wagner, D., Perry, V.H., and Coleman, M.P. (2000). A Ufd2/D4Cole1e chimeric protein and overexpression of Rbp7 in the slow Wallerian degeneration (Wld(S)) mouse. Proceedings Of The National Academy Of Sciences Of The United States Of America *97*, 11377-11382.

Conforti, L., Wilbrey, A., Morreale, G., Janeckova, L., Beirowski, B., Adalbert, R., Mazzola, F., Di Stefano, M., Hartley, R., Babetto, E., *et al.* (2009). Wld S protein requires Nmnat activity and a short N-terminal sequence to protect axons in mice. J Cell Biol *184*, 491-500.

Cragg, B.G. (1970). What is the signal for chromatolysis? Brain Research *23*, 1-21.

Dahmen, W., Webb, B., and Preiss, J. (1967). The deamido-diphosphopyridine nucleotide and diphosphopyridine nucleotide pyrophosphorylases of Escherichia coli and yeast. Arch Biochem Biophys *120*, 440-450.

de Hoop, M.J., Huber, L.A., Stenmark, H., Williamson, E., Zerial, M., Parton, R.G., and Dotti, C.G. (1994). The involvement of the small GTP-binding protein Rab5a in neuronal endocytosis. Neuron *13*, 11-22.

Dolle, C., Niere, M., Lohndal, E., and Ziegler, M. (2010). Visualization of subcellular NAD pools and intra-organellar protein localization by poly-ADP-ribose formation. Cell Mol Life Sci *67*, 433-443.

Duden, R. (2003). ER-to-Golgi transport: COP I and COP II function (Review). Mol Membr Biol *20*, 197-207.

Duden, R., Griffiths, G., Frank, R., Argos, P., and Kreis, T.E. (1991). Beta-COP, a 110 kd protein associated with non-clathrin-coated vesicles and the Golgi complex, shows homology to beta-adaptin. Cell *64*, 649-665.

El-Husseini Ael, D., Craven, S.E., Brock, S.C., and Bredt, D.S. (2001). Polarized targeting of peripheral membrane proteins in neurons. J Biol Chem *276*, 44984-44992.

Encinas, M., Iglesias, M., Liu, Y., Wang, H., Muhaisen, A., Cena, V., Gallego, C., and Comella, J.X. (2000). Sequential treatment of SH-SY5Y cells with retinoic acid and brain-derived neurotrophic factor gives rise to fully differentiated, neurotrophic factor-dependent, human neuron-like cells. J Neurochem *75*, 991-1003.

Feng, G., Mellor, R.H., Bernstein, M., Keller-Peck, C., Nguyen, Q.T., Wallace, M., Nerbonne, J.M., Lichtman, J.W., and Sanes, J.R. (2000). Imaging neuronal subsets in transgenic mice expressing multiple spectral variants of GFP. Neuron *28*, 41-51.

Feng, Y., Press, B., and Wandinger-Ness, A. (1995). Rab 7: an important regulator of late endocytic membrane traffic. J Cell Biol *131*, 1435-1452.

Feng, Y., Yan, T., Zheng, J., Ge, X., Mu, Y., Zhang, Y., Wu, D., Du, J.L., and Zhai, Q. (2010). Overexpression of Wld(S) or Nmnat2 in mauthner cells by single-cell electroporation delays axon degeneration in live zebrafish. J Neurosci Res *88*, 3319-3327.

Finkel, T., Deng, C.X., and Mostoslavsky, R. (2009). Recent progress in the biology and physiology of sirtuins. Nature *460*, 587-591.

Finn, J.T., Weil, M., Archer, F., Siman, R., Srinivasan, A., and Raff, M.C. (2000). Evidence that wallerian degeneration and localized axon degeneration induced by local neurotrophin deprivation do not involve caspases. Journal Of Neuroscience *20*, 1333-1341.

Fischer von Mollard, G., Stahl, B., Walch-Solimena, C., Takei, K., Daniels, L., Khoklatchev, A., De Camilli, P., Sudhof, T.C., and Jahn, R. (1994). Localization of Rab5 to synaptic vesicles identifies endosomal intermediate in synaptic vesicle recycling pathway. Eur J Cell Biol *65*, 319-326.

Gilley, J., and Coleman, M.P. (2010). Endogenous Nmnat2 is an essential survival factor for maintenance of healthy axons. PLoS Biol *8*, e1000300.

Giuditta, A., Tai Chun, J., Eyman, M., Cefaliello, C., Bruno, A.P., and Crispino, M. (2008). Local Gene Expression in Axons and Nerve Endings: The Glia-Neuron Unit. Physiol Rev *88*, 515-555.

Graeff, R., Liu, Q., Kriksunov, I.A., Kotaka, M., Oppenheimer, N., Hao, Q., and Lee, H.C. (2009). Mechanism of cyclizing NAD to cyclic ADP-ribose by ADP-ribosyl cyclase and CD38. J Biol Chem *284*, 27629-27636.

Griffin, J.W., George, E.B., Hsieh, S.T., and Glass, J.D. (1995). Axonal Degeneration and Disorders of the Axonal Cytoskeleton. In The Axon: Structure, Function and Pathophysiology, S.G. Waxman, J.D. Kocsis, and P.K. Stys, eds. (New York, Oxford University Press), pp. 375-390.

Griffiths, G., Pepperkok, R., Locker, J.K., and Kreis, T.E. (1995). Immunocytochemical localization of beta-COP to the ER-Golgi boundary and the TGN. J Cell Sci *108 (Pt 8)*, 2839-2856.

Guo, H., and Xiong, J. (2006). A specific and versatile genome walking technique. Gene *381*, 18-23.

Haferkamp, I., Schmitz-Esser, S., Linka, N., Urbany, C., Collingro, A., Wagner, M., Horn, M., and Neuhaus, H.E. (2004). A candidate NAD+ transporter

in an intracellular bacterial symbiont related to Chlamydiae. Nature *432*, 622-625.

Hamill, R.C. (1912). Examination of the Central Nervous System in Seven Cases of Pellagra. The Journal of Infectious Diseases *10*, 190-191.

Hegyi, J., Schwartz, R.A., and Hegyi, V. (2004). Pellagra: dermatitis, dementia, and diarrhea. Int J Dermatol *43*, 1-5.

Hildmann, C., Riester, D., and Schwienhorst, A. (2007). Histone deacetylases--an important class of cellular regulators with a variety of functions. Appl Microbiol Biotechnol *75*, 487-497.

Hirschey, M.D., Shimazu, T., Goetzman, E., Jing, E., Schwer, B., Lombard, D.B., Grueter, C.A., Harris, C., Biddinger, S., Ilkayeva, O.R., *et al.* (2010). SIRT3 regulates mitochondrial fatty-acid oxidation by reversible enzyme deacetylation. Nature *464*, 121-125.

Hogeboom, G.H., and Schneider, W.C. (1952). Cytochemical studies. VI. The synthesis of diphosphopyridine nucleotide by liver cell nuclei. J Biol Chem *197*, 611-620.

Horton, A.C., Racz, B., Monson, E.E., Lin, A.L., Weinberg, R.J., and Ehlers, M.D. (2005). Polarized secretory trafficking directs cargo for asymmetric dendrite growth and morphogenesis. Neuron *48*, 757-771.

Hottiger, M.O., Hassa, P.O., Luscher, B., Schuler, H., and Koch-Nolte, F. (2010). Toward a unified nomenclature for mammalian ADP-ribosyltransferases. Trends Biochem Sci *35*, 208-219.

Houtkooper, R.H., Canto, C., Wanders, R.J., and Auwerx, J. (2010). The secret life of NAD+: an old metabolite controlling new metabolic signaling pathways. Endocr Rev *31*, 194-223.

Huang, K., and El-Husseini, A. (2005). Modulation of neuronal protein trafficking and function by palmitoylation. Curr Opin Neurobiol *15*, 527-535.

Ikegami, K., and Koike, T. (2003). Non-apoptotic neurite degeneration in apoptotic neuronal death: Pivotal role of mitochondrial function in neurites. Neuroscience *122*, 617-626.

Imai, S., Armstrong, C.M., Kaeberlein, M., and Guarente, L. (2000). Transcriptional silencing and longevity protein Sir2 is an NAD-dependent histone deacetylase. Nature *403*, 795-800.

Ishii, N., and Nishihara, Y. (1981). Pellagra among chronic alcoholics: clinical and pathological study of 20 necropsy cases. J Neurol Neurosurg Psychiatry *44*, 209-215.

Jin, D., Liu, H.-X., Hirai, H., Torashima, T., Nagai, T., Lopatina, O., Shnayder, N.A., Yamada, K., Noda, M., Seike, T., *et al.* (2007). CD38 is critical for social behaviour by regulating oxytocin secretion. Nature *446*, 41-45.

Jones, D.H., and Matus, A.I. (1974). Isolation of synaptic plasma membrane from brain by combined flotation-sedimentation density gradient centrifugation. Biochim Biophys Acta *356*, 276-287.

Kaganovich, D., Kopito, R., and Frydman, J. (2008). Misfolded proteins partition between two distinct quality control compartments. Nature *454*, 1088-1095.

Kaneko, C., Hatakeyama, S., Matsumoto, M., Yada, M., Nakayama, K., and Nakayama, K.I. (2003). Characterization of the mouse gene for the U-box-type ubiquitin ligase UFD2a. *300*, 297.

Kang, R., Wan, J., Arstikaitis, P., Takahashi, H., Huang, K., Bailey, A.O., Thompson, J.X., Roth, A.F., Drisdel, R.C., Mastro, R., *et al.* (2008).

Neural palmitoyl-proteomics reveals dynamic synaptic palmitoylation. Nature *456*, 904-909.

Kinsella, B.T., and Maltese, W.A. (1991). rab GTP-binding proteins implicated in vesicular transport are isoprenylated in vitro at cysteines within a novel carboxyl-terminal motif. J Biol Chem *266*, 8540-8544.

Kinsella, B.T., and Maltese, W.A. (1992). rab GTP-binding proteins with three different carboxyl-terminal cysteine motifs are modified in vivo by 20-carbon isoprenoids. J Biol Chem *267*, 3940-3945.

Knaus, P., Betz, H., and Rehm, H. (1986). Expression of synaptophysin during postnatal development of the mouse brain. J Neurochem *47*, 1302-1304.

Koch-Nolte, F., Haag, F., Guse, A.H., Lund, F., and Ziegler, M. (2009). Emerging roles of NAD+ and its metabolites in cell signaling. Sci Signal *2*, mr1.

Kraus, W.L. (2008). Transcriptional control by PARP-1: chromatin modulation, enhancer-binding, coregulation, and insulation. Curr Opin Cell Biol *20*, 294-302.

Krishnakumar, R., and Kraus, W.L. (2010). The PARP side of the nucleus: molecular actions, physiological outcomes, and clinical targets. Mol Cell *39*, 8-24.

Kurnasov, O.V., Polanuyer, B.M., Ananta, S., Sloutsky, R., Tam, A., Gerdes, S.Y., and Osterman, A.L. (2002). Ribosylnicotinamide Kinase Domain of NadR Protein: Identification and Implications in NAD Biosynthesis. J Bacteriol *184*, 6906-6917.

Lansbury, P.T., and Lashuel, H.A. (2006). A century-old debate on protein aggregation and neurodegeneration enters the clinic. Nature *443*, 774-779.

Lasek, R.J., Garner, J.A., and Brady, S.T. (1984). Axonal transport of the cytoplasmic matrix. J Cell Biol *99*, 212s-221s.

Lau, C., Dolle, C., Gossmann, T.I., Agledal, L., Niere, M., and Ziegler, M. (2010). Isoform-specific targeting and interaction domains in human nicotinamide mononucleotide adenylyltransferases. J Biol Chem *285*, 18868-18876.

Lau, C., Niere, M., and Ziegler, M. (2009). The NMN/NaMN adenylyltransferase (NMNAT) protein family. Front Biosci *14*, 410-431.

Lin, S.J., Ford, E., Haigis, M., Liszt, G., and Guarente, L. (2004). Calorie restriction extends yeast life span by lowering the level of NADH. Genes & Development *18*, 12-16.

Lowe, G., and Tansley, G. (1983). The stereochemical course of nucleotidyl transfer catalysed by NAD pyrophosphorylase. Eur J Biochem *132*, 117-120.

Lubinska, L. (1982). Patterns of Wallerian degeneration of myelinated fibres in short and long peripheral stumps and in isolated segments of rat phrenic nerve. Interpretation of the role of axoplasmic flow of the trophic factor. Brain Research *233*, 227-240.

Lunn, E.R., Perry, V.H., Brown, M.C., Rosen, H., and Gordon, S. (1989). Absence of Wallerian Degeneration does not Hinder Regeneration in Peripheral Nerve. Eur J Neurosci *1*, 27-33.

Lyon, M.F., Ogunkolade, B.W., Brown, M.C., Atherton, D.J., and Perry, V.H. (1993). A Gene Affecting Wallerian Nerve Degeneration Maps Distally On Mouse Chromosome-4. Proceedings Of The National Academy Of Sciences Of The United States Of America *90*, 9717-9720.

Mack, T.G., Reiner, M., Beirowski, B., Mi, W., Emanuelli, M., Wagner, D., Thomson, D., Gillingwater, T., Court, F., Conforti, L., *et al.* (2001). Wallerian degeneration of injured axons and synapses is delayed by a Ube4b/Nmnat chimeric gene. Nat Neurosci *4*, 1199-1206.

Magni, G., Amici, A., Emanuelli, M., Orsomando, G., Raffaelli, N., and Ruggieri, S. (2004). Enzymology of NAD+ homeostasis in man. Cell Mol Life Sci *61*, 19-34.

Magni, G., Amici, A., Emanuelli, M., Raffaelli, N., and Ruggieri, S. (1999). Enzymology of NAD+ synthesis. Adv Enzymol Relat Areas Mol Biol *73*, 135-182, xi.

Magni, G., Orsomando, G., Raffelli, N., and Ruggieri, S. (2008). Enzymology of mammalian NAD metabolism in health and disease. Front Biosci *13*, 6135-6154.

Maximov, A., Shin, O.H., Liu, X., and Sudhof, T.C. (2007). Synaptotagmin-12, a synaptic vesicle phosphoprotein that modulates spontaneous neurotransmitter release. J Cell Biol *176*, 113-124.

Mayer, P.R., Huang, N., Dewey, C.M., Dries, D.R., Zhang, H., and Yu, G. (2010). Expression, localization and biochemical characterization of NMN adenylyltransferase 2. J Biol Chem.

Mu, F.T., Callaghan, J.M., Steele-Mortimer, O., Stenmark, H., Parton, R.G., Campbell, P.L., McCluskey, J., Yeo, J.P., Tock, E.P., and Toh, B.H. (1995). EEA1, an early endosome-associated protein. EEA1 is a conserved alpha-helical peripheral membrane protein flanked by cysteine "fingers" and contains a calmodulin-binding IQ motif. J Biol Chem *270*, 13503-13511.

Nakahata, Y., Sahar, S., Astarita, G., Kaluzova, M., and Sassone-Corsi, P. (2009). Circadian control of the NAD+ salvage pathway by CLOCK-SIRT1. Science *324*, 654-657.

Nakamura, N., Rabouille, C., Watson, R., Nilsson, T., Hui, N., Slusarewicz, P., Kreis, T.E., and Warren, G. (1995). Characterization of a cis-Golgi matrix protein, GM130. J Cell Biol *131*, 1715-1726.

Noritake, J., Fukata, Y., Iwanaga, T., Hosomi, N., Tsutsumi, R., Matsuda, N., Tani, H., Iwanari, H., Mochizuki, Y., Kodama, T., *et al.* (2009). Mobile

DHHC palmitoylating enzyme mediates activity-sensitive synaptic targeting of PSD-95. The Journal of Cell Biology *186*, 147-160.

Ohno, Y., Kihara, A., Sano, T., and Igarashi, Y. (2006). Intracellular localization and tissue-specific distribution of human and yeast DHHC cysteine-rich domain-containing proteins. Biochimica et Biophysica Acta (BBA) - Molecular and Cell Biology of Lipids *1761*, 474-483.

Oprins, A., Duden, R., Kreis, T.E., Geuze, H.J., and Slot, J.W. (1993). Beta-COP localizes mainly to the cis-Golgi side in exocrine pancreas. J Cell Biol *121*, 49-59.

Perin, M.S., Fried, V.A., Mignery, G.A., Jahn, R., and Sudhof, T.C. (1990). Phospholipid binding by a synaptic vesicle protein homologous to the regulatory region of protein kinase C. Nature *345*, 260-263.

Perry, V.H., Lunn, E.R., Brown, M.C., Cahusac, S., and Gordon, S. (1990). Evidence that the Rate of Wallerian Degeneration is Controlled by a Single Autosomal Dominant Gene. Eur J Neurosci *2*, 408-413.

Ponnambalam, S., Girotti, M., Yaspo, M.L., Owen, C.E., Perry, A.C., Suganuma, T., Nilsson, T., Fried, M., Banting, G., and Warren, G. (1996). Primate

homologues of rat TGN38: primary structure, expression and functional implications. J Cell Sci *109 (Pt 3)*, 675-685.

Preiss, J., and Handler, P. (1958). Biosynthesis of diphosphopyridine nucleotide. II. Enzymatic aspects. J Biol Chem *233*, 493-500.

Press, C., and Milbrandt, J. (2008). Nmnat delays axonal degeneration caused by mitochondrial and oxidative stress. J Neurosci *28*, 4861-4871.

Raff, M.C., Whitmore, A.V., and Finn, J.T. (2002). Axonal self-destruction and neurodegeneration. Science *296*, 868-871.

Raffaelli, N., Sorci, L., Amici, A., Emanuelli, M., Mazzola, F., and Magni, G. (2002). Identification of a novel human nicotinamide mononucleotide adenylyltransferase. Biochem Biophys Res Commun *297*, 835-840.

Ramsey, K.M., Yoshino, J., Brace, C.S., Abrassart, D., Kobayashi, Y., Marcheva, B., Hong, H.K., Chong, J.L., Buhr, E.D., Lee, C., *et al.* (2009). Circadian clock feedback cycle through NAMPT-mediated NAD+ biosynthesis. Science *324*, 651-654.

Resh, M.D. (2006). Trafficking and signaling by fatty-acylated and prenylated proteins. Nat Chem Biol *2*, 584-590.

Revollo, J.R., Grimm, A.A., and Imai, S. (2004). The NAD biosynthesis pathway mediated by nicotinamide phosphoribosyltransferase regulates Sir2 activity in mammalian cells. J Biol Chem *279*, 50754-50763.

Rocks, O., Gerauer, M., Vartak, N., Koch, S., Huang, Z.P., Pechlivanis, M., Kuhlmann, J., Brunsveld, L., Chandra, A., Ellinger, B., *et al.* (2010). The palmitoylation machinery is a spatially organizing system for peripheral membrane proteins. Cell *141*, 458-471.

Rodgers, J.T., Lerin, C., Haas, W., Gygi, S.P., Spiegelman, B.M., and Puigserver, P. (2005). Nutrient control of glucose homeostasis through a complex of PGC-1alpha and SIRT1. Nature *434*, 113-118.

Salmon, P., and Trono, D. (2006). Production and titration of lentiviral vectors. Curr Protoc Neurosci *Chapter 4*, Unit 4 21.

Sannerud, R., Marie, M., Nizak, C., Dale, H.A., Pernet-Gallay, K., Perez, F., Goud, B., and Saraste, J. (2006). Rab1 defines a novel pathway connecting

the pre-Golgi intermediate compartment with the cell periphery. Mol Biol Cell *17*, 1514-1526.

Saridakis, V., Christendat, D., Kimber, M.S., Dharamsi, A., Edwards, A.M., and Pai, E.F. (2001). Insights into ligand binding and catalysis of a central step in NAD+ synthesis: structures of Methanobacterium thermoautotrophicum NMN adenylyltransferase complexes. J Biol Chem *276*, 7225-7232.

Sasaki, Y., Araki, T., and Milbrandt, J. (2006). Stimulation of nicotinamide adenine dinucleotide biosynthetic pathways delays axonal degeneration after axotomy. J Neurosci *26*, 8484-8491.

Sasaki, Y., and Milbrandt, J. (2010). Axonal degeneration is blocked by nicotinamide mononucleotide adenylyltransferase (NMNAT) protein transduction into transected axons. J Biol Chem.

Sastry, L., Johnson, T., Hobson, M.J., Smucker, B., and Cornetta, K. (2002). Titering lentiviral vectors: comparison of DNA, RNA and marker expression methods. Gene Ther *9*, 1155-1162.

Sauve, A.A. (2010). Sirtuin chemical mechanisms. Biochim Biophys Acta *1804*, 1591-1603.

Sauve, A.A., Moir, R.D., Schramm, V.L., and Willis, I.M. (2005). Chemical activation of Sir2-dependent silencing by relief of nicotinamide inhibition. Mol Cell *17*, 595-601.

Schoch, S., Deak, F., Konigstorfer, A., Mozhayeva, M., Sara, Y., Sudhof, T.C., and Kavalali, E.T. (2001). SNARE function analyzed in synaptobrevin/VAMP knockout mice. Science *294*, 1117-1122.

Schuber, F., and Lund, F.E. (2004). Structure and enzymology of ADP-ribosyl cyclases: conserved enzymes that produce multiple calcium mobilizing metabolites. Curr Mol Med *4*, 249-261.

Schweiger, M., Hennig, K., Lerner, F., Niere, M., Hirsch-Kauffmann, M., Specht, T., Weise, C., Oei, S.L., and Ziegler, M. (2001). Characterization of recombinant human nicotinamide mononucleotide adenylyl transferase (NMNAT), a nuclear enzyme essential for NAD synthesis. FEBS Lett *492*, 95-100.

Schwer, B., and Verdin, E. (2008). Conserved metabolic regulatory functions of sirtuins. Cell Metab *7*, 104-112.

Shatton, J.B., Williams, A., and Weinhouse, S. (1983). Subcellular distribution of inorganic pyrophosphatase activity in various normal and neoplastic cell types. Cancer Res *43*, 3742-3747.

Shaw, G., and Weber, K. (1982). Differential expression of neurofilament triplet proteins in brain development. Nature *298*, 277-279.

Sheffield, P., Garrard, S., and Derewenda, Z. (1999). Overcoming expression and purification problems of RhoGDI using a family of "parallel" expression vectors. Protein Expr Purif *15*, 34-39.

Shibata, K., Hayakawa, T., and Iwai, K. (1986). Tissue Distribution of the Enzymes Concerned with the Biosynthesis of NAD in Rats(Biological Chemistry). Agricultural and biological chemistry *50*, 3037-3041.

Smith, B.C., Hallows, W.C., and Denu, J.M. (2008). Mechanisms and molecular probes of sirtuins. Chem Biol *15*, 1002-1013.

Soler-Llavina, G.J., and Sabatini, B.L. (2006). Synapse-specific plasticity and compartmentalized signaling in cerebellar stellate cells. Nat Neurosci *9*, 798-806.

Sood, R., Bonner, T.I., Makalowska, I., Stephan, D.A., Robbins, C.M., Connors, T.D., Morgenbesser, S.D., Su, K., Faruque, M.U., Pinkett, H., *et al.* (2001). Cloning and characterization of 13 novel transcripts and the human RGS8 gene from the 1q25 region encompassing the hereditary prostate cancer (HPC1) locus. Genomics *73*, 211-222.

Sorci, L., Cimadamore, F., Scotti, S., Petrelli, R., Cappellacci, L., Franchetti, P., Orsomando, G., and Magni, G. (2007). Initial-rate kinetics of human NMN-adenylyltransferases: substrate and metal ion specificity, inhibition by products and multisubstrate analogues, and isozyme contributions to NAD+ biosynthesis. Biochemistry *46*, 4912-4922.

Spies, T.D., Bean, W.B., and Ashe, W.F. (1939). RECENT ADVANCES IN THE TREATMENT OF PELLAGRA AND ASSOCIATED DEFICIENCIES*. Annals of Internal Medicine *12*, 1830-1844.

Stenmark, H. (2009). Rab GTPases as coordinators of vesicle traffic. Nat Rev Mol Cell Biol *10*, 513-525.

Takamori, S., Holt, M., Stenius, K., Lemke, E.A., Gronborg, M., Riedel, D., Urlaub, H., Schenck, S., Brugger, B., Ringler, P., *et al.* (2006). Molecular anatomy of a trafficking organelle. Cell *127*, 831-846.

Vargas, M.E., and Barres, B.A. (2007). Why is Wallerian degeneration in the CNS so slow? Annu Rev Neurosci *30*, 153-179.

Vavouri, T., Semple, J.I., Garcia-Verdugo, R., and Lehner, B. (2009). Intrinsic protein disorder and interaction promiscuity are widely associated with dosage sensitivity. Cell *138*, 198-208.

Voss, A.K., Thomas, T., and Gruss, P. (1998a). Compensation for a gene trap mutation in the murine microtubule-associated protein 4 locus by alternative polyadenylation and alternative splicing. Dev Dyn *212*, 258-266.

Voss, A.K., Thomas, T., and Gruss, P. (1998b). Efficiency assessment of the gene trap approach. Dev Dyn *212*, 171-180.

Waller, A. (1850). Experiments on the Section of the Glossopharyngeal and Hypoglossal Nerves of the Frog, and Observations of the Alterations

Produced Thereby in the Structure of Their Primitive Fibres. Philosophical Transactions of the Royal Society of London *140*, 423-429.

Wang, Q., Song, C., and Li, C.C. (2004). Molecular perspectives on p97-VCP: progress in understanding its structure and diverse biological functions. J Struct Biol *146*, 44-57.

Whitmore, A.V., Lindsten, T., Raff, M.C., and Thompson, C.B. (2003). The proapoptotic proteins Bax and Bak are not involved in Wallerian degeneration. Cell Death And Differentiation *10*, 260-261.

Whittaker, V.P. (1993). Thirty years of synaptosome research. J Neurocytol *22*, 735-742.

Whittaker, V.P., Michaelson, I.A., and Kirkland, R.J. (1964). The separation of synaptic vesicles from nerve-ending particles ('synaptosomes'). Biochem J *90*, 293-303.

Yalowitz, J.A., Xiao, S., Biju, M.P., Antony, A.C., Cummings, O.W., Deeg, M.A., and Jayaram, H.N. (2004). Characterization of human brain nicotinamide 5'-mononucleotide adenylyltransferase-2 and expression in human pancreas. Biochem J *377*, 317-326.

Yamada, K., Hara, N., Shibata, T., Osago, H., and Tsuchiya, M. (2006). The simultaneous measurement of nicotinamide adenine dinucleotide and related compounds by liquid chromatography/electrospray ionization tandem mass spectrometry. Anal Biochem *352*, 282-285.

Yan, T., Feng, Y., Zheng, J., Ge, X., Zhang, Y., Wu, D., Zhao, J., and Zhai, Q. (2009). Nmnat2 delays axon degeneration in superior cervical ganglia dependent on its NAD synthesis activity. Neurochem Int.

Yang, H., Yang, T., Baur, J.A., Perez, E., Matsui, T., Carmona, J.J., Lamming, D.W., Souza-Pinto, N.C., Bohr, V.A., Rosenzweig, A., *et al.* (2007). Nutrient-sensitive mitochondrial NAD+ levels dictate cell survival. Cell *130*, 1095-1107.

Yu, J., and Auwerx, J. (2009). The role of sirtuins in the control of metabolic homeostasis. Ann N Y Acad Sci *1173 Suppl 1*, E10-19.

Yu, S.W., Wang, H., Poitras, M.F., Coombs, C., Bowers, W.J., Federoff, H.J., Poirier, G.G., Dawson, T.M., and Dawson, V.L. (2002). Mediation of poly(ADP-ribose) polymerase-1-dependent cell death by apoptosis-inducing factor. Science *297*, 259-263.

Zhai, R.G., Cao, Y., Hiesinger, P.R., Zhou, Y., Mehta, S.Q., Schulze, K.L., Verstreken, P., and Bellen, H.J. (2006). Drosophila NMNAT maintains neural integrity independent of its NAD synthesis activity. PLoS Biol *4*, e416.

Zhang, T., Berrocal, J.G., Frizzell, K.M., Gamble, M.J., DuMond, M.E., Krishnakumar, R., Yang, T., Sauve, A.A., and Kraus, W.L. (2009). Enzymes in the NAD+ salvage pathway regulate SIRT1 activity at target gene promoters. J Biol Chem *284*, 20408-20417.

Zhang, X., Kurnasov, O.V., Karthikeyan, S., Grishin, N.V., Osterman, A.L., and Zhang, H. (2003). Structural characterization of a human cytosolic NMN/NaMN adenylyltransferase and implication in human NAD biosynthesis. J Biol Chem *278*, 13503-13511.

Zhong, L., D'Urso, A., Toiber, D., Sebastian, C., Henry, R.E., Vadysirisack, D.D., Guimaraes, A., Marinelli, B., Wikstrom, J.D., Nir, T., *et al.* (2010). The histone deacetylase Sirt6 regulates glucose homeostasis via Hif1alpha. Cell *140*, 280-293.